CT of the Neck: Image Analysis and Reporting in the Emergency Setting

Alain Cunqueiro, MD
William A. Gomes, MD, PhD
Peter Lee, MD
R. Joshua Dym, MD
Meir H. Scheinfeld, MD, PhD

Abbreviations: EAC = external auditory canal, PTA = peritonsillar abscess

RadioGraphics 2019; 39:1760–1781

https://doi.org/10.1148/rg.2019190012

Content Codes: CT ER HN IN NR

From the Division of Emergency Radiology (M.H.S.), Department of Radiology (A.C., P.L.), Montefiore Medical Center, Albert Einstein College of Medicine, 111 E 210 St, Bronx, NT 10467; Department of Radiology, Westchester Medical Center, Valhalla, NY (W.A.G.); and Department of Radiology, Rutgers New Jersey Medical School, Newark, NJ (R.J.D.). Presented as an education exhibit at the 2018 RSNA Annual Meeting. Received February 25, 2019; revision requested March 28 and received April 1; accepted April 11. For this journal-based SA-CME activity, the authors, editor, and reviewers have disclosed no relevant relationships. **Address correspondence to** M.H.S. (e-mail: *mscheinf@montefiore.org*).

SA-CME LEARNING OBJECTIVES

After completing this journal-based SA-CME activity, participants will be able to:

- Describe how to systematically interpret the findings of neck CT performed in the emergency department.
- Identify common pathologic entities found at neck CT in the emergency department.
- Compose a report detailing and synthesizing the findings seen at emergency neck CT.

See rsna.org/learning-center-rg.

Interpreting findings seen at CT of the neck is challenging owing to the complex and nuanced anatomy of the neck, which contains multiple organ systems in a relatively small area. In the emergency department setting, CT is performed to investigate acute infectious or inflammatory symptoms and chronic processes. With few exceptions, neck CT should be performed with intravenous contrast material, which accentuates abnormally enhancing phlegmonous and neoplastic tissues and can be used to delineate any abscesses or necrotic areas. As part of the evaluation, the vascular structures and aerodigestive tract must be scrutinized, particularly for patency. Furthermore, although the patient may present because of symptoms that suggest non–life-threatening conditions involving structures such as the teeth or salivary glands, there may be serious implications for other areas, such as the orbits, brain, and spinal cord, that also may be revealed at the examination. With a focus on the emergency setting, the authors propose using an approach to interpreting neck CT findings whereby 12 areas are systematically evaluated and reported on: the cutaneous and subcutaneous soft tissues, aerodigestive tract and adjacent soft tissues, teeth and periodontal tissues, thyroid gland, salivary glands, lymph nodes, vascular structures, bony airspaces, cervical spine, orbits and imaged brain, lung apices, and superior mediastinum. The use of a systematic approach to interpreting neck CT findings is essential for identifying all salient findings, recognizing and synthesizing the implications of these findings to formulate the correct diagnosis, and reporting the findings and impressions in a complete, clear, and logical manner.

Online supplemental material is available for this article.

Introduction

In the emergency setting, CT of the neck is often performed to investigate symptoms of acute infection or inflammation or symptoms of aerodigestive tract compromise referable to the neck. A neck mass or adenopathy also may be investigated, particularly when it results in airway or vascular compromise. In a recent single-center study (1), neck CT had a positivity rate of 87%, indicating that it is generally performed for good reason and, therefore, imaging findings should be expected. Interpretation of neck CT findings can be challenging, primarily because of the multiple organ systems in the neck. Because there are components of the respiratory, digestive, vascular, endocrine, skeletal, and neurologic systems in the neck, the radiologist is required to have knowledge and an understanding of how disease manifests and how an abnormality in one system can spread and affect other systems.

TEACHING POINTS

- A checklist approach similar to that used for interpreting abdominopelvic CT images, in which all imaged organs such as the lung bases, heart, liver, gallbladder, biliary tree, spleen, pancreas, adrenal glands, and other organs are systematically evaluated, also seems prudent for interpreting neck CT images.
- CT images in patients with epiglottitis show thickening of the mucosa of the epiglottis, aryepiglottic folds, and/or arytenoids. As the epithelium is tightly bound to the vocal cords, edema does not spread inferior to them. Also, because the epithelium and lamina propria are loosely bound to the epiglottic cartilage on the lingual side, there may be initial thickening of only the anterior surface.
- With Ludwig angina, CT images show inflammatory stranding and fluid in the submandibular and sublingual spaces, with or without abscesses or gas. As Ludwig angina is a "cellulitis," rim-enhancing components are not required to make the diagnosis.
- An intracranial aneurysm is a particularly important finding that may be incidentally encountered at neck CT. The prevalence of intracranial aneurysm in the general population without comorbidities has been estimated to be 3.2%. Owing to the risk of aneurysmal rupture with devastating subarachnoid hemorrhage and the availability of effective treatment options, the intracranial arteries should be scrutinized in every case.
- Epidural abscesses are collections of pus in the epidural space and are most commonly due to sinus infections. CT images show a rim-enhancing collection with characteristics of an epidural collection (eg, lentiform in shape, usually not crossing sutures). When these abscesses result from a temporal bone infection such as mastoiditis, a rim-enhancing epidural collection may be seen between the mastoid bone and the cerebellum or temporal lobe.

The traditional approach to neck CT analysis is focused on an understanding of the fascial spaces of the neck (2–4). Knowledge of this complex anatomy is necessary when a mass or inflammatory process is identified, and a strategy for determining which structures are deviated and the direction of the deviations must be used to make a diagnosis or differential diagnosis. Still, having a systematic approach to evaluating the common locations of disease is beneficial for efficient and consistent detection of all salient imaging findings. A checklist approach similar to that used for interpreting abdominopelvic CT images, in which all imaged organs such as the lung bases, heart, liver, gallbladder, biliary tree, spleen, pancreas, and adrenal glands are systematically evaluated, also seems prudent for interpreting neck CT images.

In this article, we describe a 12-item checklist-based approach, informed by the space-based approach, that can be used to address the complex anatomy and variety of possible abnormalities that can be seen in the nontraumatic emergency setting (Table). It should be emphasized that once a specific disease process is suspected, its pathophysiologic features should be used to guide the search for other areas of involvement and validate or reject the suspicion. Ultimately, individual findings must be synthesized to derive a diagnosis or differential diagnosis that can guide further management.

Twelve Areas of Assessment on the Neck CT Analysis Checklist

1. Cutaneous and subcutaneous soft tissues
2. Aerodigestive tract and adjacent soft tissues
3. Teeth and periodontal tissues
4. Thyroid gland
5. Salivary glands
6. Lymph nodes
7. Vascular structures
8. Bony airspaces
9. Cervical spine
10. Orbits and imaged brain
11. Lung apices
12. Superior mediastinum

We begin by describing a protocol for CT of the neck. Then, for each item on the checklist, we describe the structures being evaluated and common (and some uncommon but important) pathologic conditions that are seen in the acute setting. We conclude by describing an approach to integrating the findings of the individual checklist items to derive a coherent diagnosis, which is reported in the "Impression" section of the report.

Neck CT Protocol

Whenever possible, neck CT should be performed with intravenous contrast material to maximize the ability to detect and characterize abscesses, masses, and vascular complications of infectious, inflammatory, and neoplastic conditions. As an exception, contrast material is not required to identify a suspected retained aerodigestive tract foreign body (5). In fact, contrast material may obscure or confound the detection of a small foreign body. Therefore, at many institutions, intravenous contrast material is not administered for this indication. When there is a palpable or focal abnormality, the CT technologist places a BB marker on that area.

At our institution, when contrast material is administered, we use a biphasic contrast agent injection protocol to achieve good parenchymal and vascular opacification, although a monophasic protocol also can be used. Sixty milliliters of iodinated contrast material is injected at 2 mL/sec for 30 seconds. Following a 60-second delay, an additional 40 mL of the agent is administered at 2 mL/sec for 20 seconds. Following a 10-second delay,

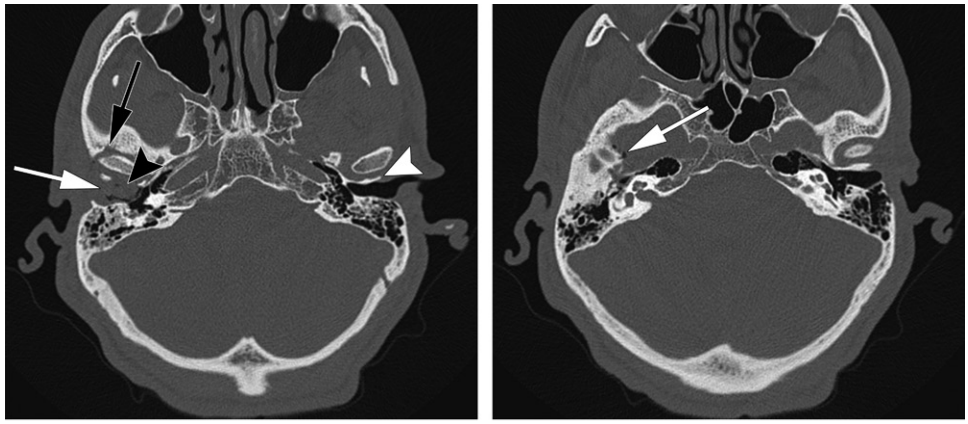

a. b.

Figure 1. Malignant otitis externa of the right ear in a 55-year-old man. **(a)** Axial nonenhanced CT image shows an opacified right EAC (white arrow). There is bone erosion of the anterior wall of the right EAC, which is also the posterior wall of the temporomandibular joint (black arrowhead). In comparison, the left anterior wall of the left EAC (white arrowhead) is complete. There is also erosion of the anterior margin of the glenoid fossa (black arrow). **(b)** Axial nonenhanced CT image obtained superior to **a** shows foci of gas (arrow) in the right middle cranial fossa.

imaging is commenced. CT images are acquired helically, from the orbital roofs to the aortic arch, by using 120 kVp and 100–300 mA, with the exact tube current varying according to patient factors. Images with a thickness of 2.5 mm are constructed in the axial, sagittal, and coronal planes by using a soft-tissue kernel and in the axial plane by using a bone kernel. Axial 0.625-mm images constructed by using bone and soft-tissue kernels also are sent to the picture archiving and communication system.

Neck CT Checklist

Cutaneous and Subcutaneous Soft Tissues

The cutaneous and subcutaneous soft tissues include the skin, subcutaneous fat, and superficial muscles (eg, platysma muscle and facial expression muscles). The subcutaneous tissues may be the primary site of inflammation or an indication of adjacent inflammation. Primary cellulitis of the subcutaneous tissues of the face may be caused by disruption of the skin due to chronic skin conditions (such as eczema and psoriasis), infection of a hair follicle (folliculitis), a retained foreign body, or minimal trauma. On CT images, the subcutaneous fat and muscular structures should have sharp definition without infiltration of the subcutaneous fat.

At CT, cellulitis manifests as skin thickening and infiltration of the subcutaneous fat and is sometimes associated with abscess formation, which appears as a rim-enhancing fluid collection (Fig E1). Thickening of the platysma muscle is commonly seen secondary to inflammation or infection of adjacent structures and serves as a beacon to draw attention to the adjacent area. Injectable filler agents such as collagen, silicone, and hyaluronic acid can mimic subcutaneous infection or inflammation, and this possibility should be considered when isolated subcutaneous infiltration or highly symmetric infiltration is detected (6).

Otitis externa, also called swimmer's ear, is a superficial infection of the external auditory canal (EAC) that is related to minor trauma or liquid exposure such as that from swimming. It is seen most commonly in children and manifests as pain, discharge, and edema of the ear canal. Although the diagnosis is usually made by means of physical examination, otitis externa manifests at contrast material–enhanced neck CT as thickening of the EAC and pinna without involvement of the underlying bone (Fig E2).

With malignant otitis externa, the more severe and invasive form of otitis externa, aggressive infection of the EAC penetrates into the adjacent bone, causing osteomyelitis of the bony EAC, temporomandibular joint, adjacent parts of the temporal bone, and skull base, with involvement of the adjacent soft tissues (7). Malignant otitis externa is a life-threatening disease that is typically seen in elderly patients with diabetes, and it is caused by *Pseudomonas aeruginosa* infection in more than 90% of cases (8). Owing to the permeative nature of this process, it may mimic a tumor (9).

Contrast-enhanced CT of malignant otitis externa will reveal extension of the infection to the bone and soft tissue outside of the EAC, with bone erosion of the EAC; soft-tissue infiltration of the infratemporal fossa; erosion, widening, and infiltration of the temporomandibular joint; soft-tissue infiltration along the eustachian tube and within the nasopharynx; and bone erosion within the petrous apex and mastoid process (Fig 1) (7,10). Among the cranial nerves, the facial nerve

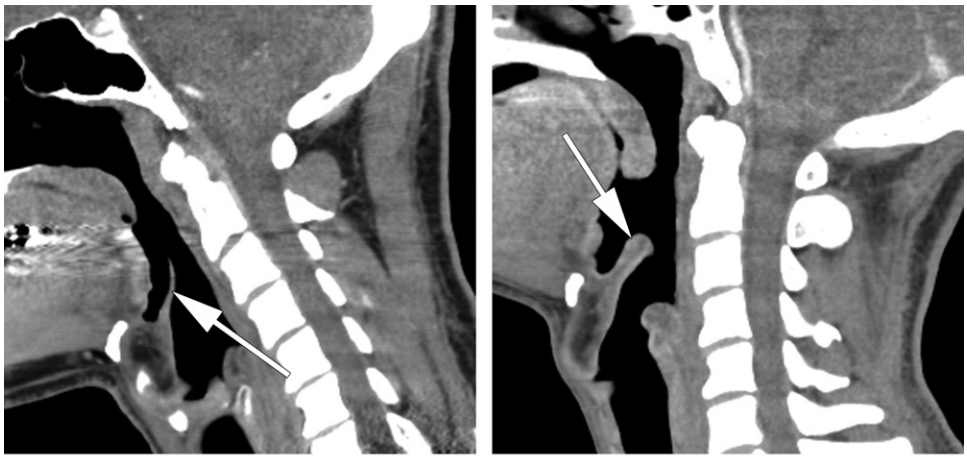

a. b.

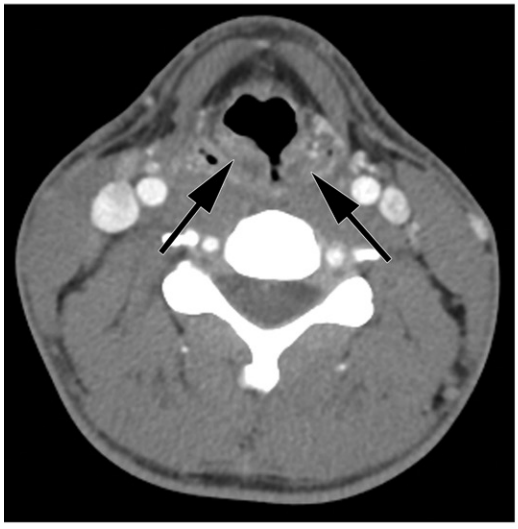

c.

Figure 2. Normal epiglottis versus epiglottitis in two patients. **(a)** Sagittal contrast-enhanced CT image in a 41-year-old man shows a normal epiglottis (arrow) measuring 2–3 mm in thickness. **(b, c)** Sagittal **(b)** and axial **(c)** contrast-enhanced CT images in a 21-year-old man with epiglottitis show thickening of the epiglottis (arrow in **b**) and aryepiglottic folds (arrows in **c**).

is the most commonly affected owing to involvement at the stylomastoid foramen. Cranial nerves V, VI, and IX–XII also may be affected as infection spreads in the soft tissues (7). Rare intracranial manifestations include sigmoid sinus thrombosis, meningitis, and brain abscess. Therefore, when a soft-tissue abnormality is detected in the EAC, adjacent bone, soft tissue, and intracranial structures should be examined for the possibility of contiguous spread.

Branchial cleft anomalies can manifest as a cyst where there is no internal or external connection, as a sinus where there is only an external connection, or as a fistula where there are openings on the skin and pharyngeal surfaces (11). Second branchial cleft anomalies account for 95% of these anomalies, and cysts are the most common anomaly at this location (11). The classic location of second branchial cleft anomalies is anterior to the sternocleidomastoid muscle, at the angle of the mandible; however, different types may manifest along a line between the oropharynx and the supraclavicular region (11). When a branchial cleft anomaly is not infected, it appears at CT as a fluid-attenuation cyst with a thin wall (12). When it is infected, the wall thickens and demonstrates contrast enhancement, and surrounding inflammatory fat stranding develops (12).

Aerodigestive Tract and Adjacent Soft Tissues

The aerodigestive tract and surrounding soft tissues must be evaluated from the mouth through the most caudal imaged portions of the esophagus and trachea. Evaluating these structures in a systematic manner, from the superior to inferior aspect, ensures that all findings will be identified. From a practical standpoint, this entails examination of the nasal cavity and nasopharynx, oral cavity and oropharynx, hypopharynx, larynx, and imaged portions of the trachea and esophagus.

At imaging, the epiglottis and aryepiglottic folds should be thin (Fig 2). There should be no thickening of the mucosa of the aerodigestive tract and no adjacent collections. Although mucosal and other types of neoplasms may be discovered incidentally, even in the acute setting (1), neoplastic disease of the neck is beyond the scope of this review and is well covered elsewhere (13–15). An important reminder regarding the imaging of all airway lesions is that imaging should not delay definitive airway management for patients with tenuous airways.

Epiglottitis and *supraglottitis* refer to life-threatening acute inflammation of the epiglottis, aryepiglottic folds, and/or arytenoids. Although

classically thought of as a disease of children, epiglottitis also affects adults, being most famously the likely cause of the death of George Washington in 1799 (16). Since the advent of the *Haemophilus influenzae* type B vaccine, there has been a dramatic reduction in epiglottitis cases among children. Epiglottitis is now more commonly seen in adults, with an incidence of one to two cases per 100 000 adults, as a result of other bacterial (*Streptococcus pneumoniae*), viral (herpes simplex), and fungal infections, or noninfectious causes such as trauma or chemicals (17,18).

Children with epiglottitis generally are in respiratory distress when they present and are diagnosed at clinical or radiographic examination. In adults who present with symptoms such as severe sore throat, dysphagia, and fever, with a more gradual onset, CT can be performed as the initial imaging investigation. CT images in patients with epiglottitis show thickening of the mucosa of the epiglottis, aryepiglottic folds, and/or arytenoids (Fig 2). As the epithelium is tightly bound to the vocal cords, edema does not spread inferior to them (16). Also, because the epithelium and lamina propria are loosely bound to the epiglottic cartilage on the lingual side, there may be initial thickening of only the anterior surface (Fig E3).

With epiglottitis, in adults in particular, only some of the supraglottic structures may be thickened (Fig E4). Identification of an epiglottic abscess increases the risk of airway obstruction, so one should carefully search for this finding (16,19).

A peritonsillar abscess (PTA) or peritonsillar phlegmon develops following tonsillitis or pharyngitis and is the most common pediatric head and neck abscess (20). A PTA is an accumulation of pus in the loose tissue around the palatine tonsil. This accumulation is due to the spread of infection from the tonsil or the obstruction of Weber glands, which are minor salivary glands that lie superior to the palatine tonsils (20). The abscess or phlegmon most commonly develops superior to the palatine tonsil, between the capsule of the tonsil (which lies medial to the abscess) and the superior pharyngeal constrictor muscle (which lies peripheral to the abscess) (21). CT can depict a spectrum of tonsillar and peritonsillar abnormalities. In tonsillitis, the tonsils are enlarged and demonstrate a striated enhancement pattern (Fig 3). Peritonsillar phlegmon appears as a vague hypoenhancing area without a well-formed rim of enhancement.

CT is 100% sensitive and 75% specific for detection of PTA, which on CT images most commonly appears as a rim-enhancing collection superolateral to the palatine tonsil (Fig 4) (21).

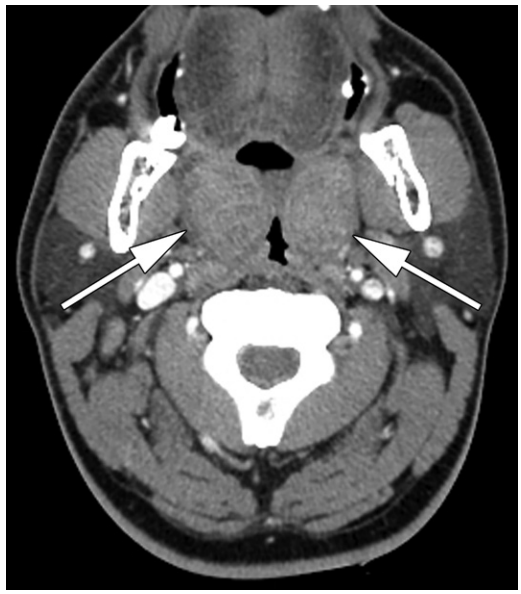

Figure 3. Tonsillitis in a 34-year-old man. Axial contrast-enhanced CT image shows enlarged palatine tonsils (arrows) that are in contact with each other ("kissing" tonsils) at the midline. The classic striated enhancement pattern is seen in the right tonsil.

When possible, a PTA should be differentiated from an intratonsillar abscess, which may not require drainage and is associated with a lower recurrence rate (22). Also, when the carotid artery has a medial course, this variant should be noted because it may be mistaken clinically for tonsil-related disease, or the artery may be injured in a tonsillar intervention (23). Therefore, we recommended documenting the distance from the closest margin of the abscess to the carotid artery and whether there are any trajectories that are particularly safe or unsafe if an intraoral drainage is performed.

Retropharyngeal abscess is an accumulation of pus posterior to the pharynx, with the potential to spread inferiorly into the mediastinum via the "danger" space. The danger space is a potential space that extends from the skull base to the diaphragm. It is bound by the alar fascia anteriorly and the prevertebral fascia posteriorly (discussed in greater detail in the "Superior Mediastinum" section) (24). In children, most commonly those between the ages of 2 and 4 years, retropharyngeal abscess is due to an upper respiratory infection or otitis that leads to enlarged lateral retropharyngeal nodes, which lie between the distal cervical internal carotid artery laterally and the prevertebral musculature medially (Fig 5), with subsequent suppuration and intranodal abscess formation (25).

If the infected nodes rupture, a retropharyngeal abscess forms. Because these lymph nodes atrophy before puberty, retropharyngeal abscess

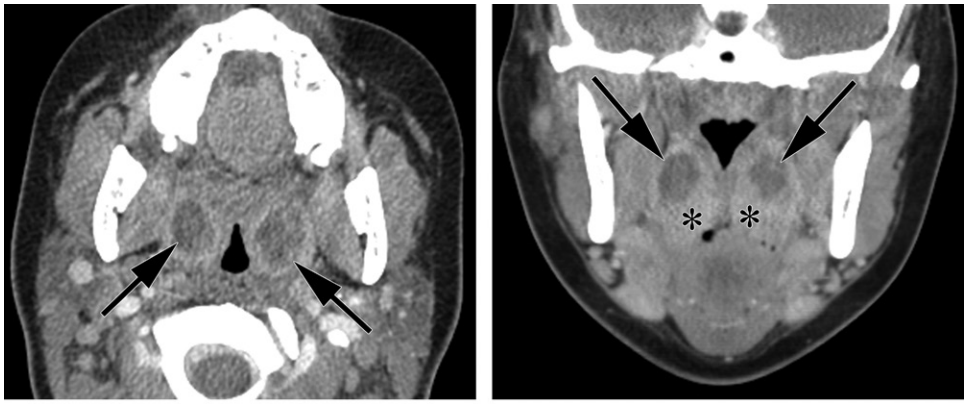

a. b.

Figure 4. Bilateral PTAs in a 21-year-old woman. Axial **(a)** and coronal **(b)** contrast-enhanced CT images show bilateral low-attenuation collections (arrows) superolateral to the palatine tonsils (* in **b**).

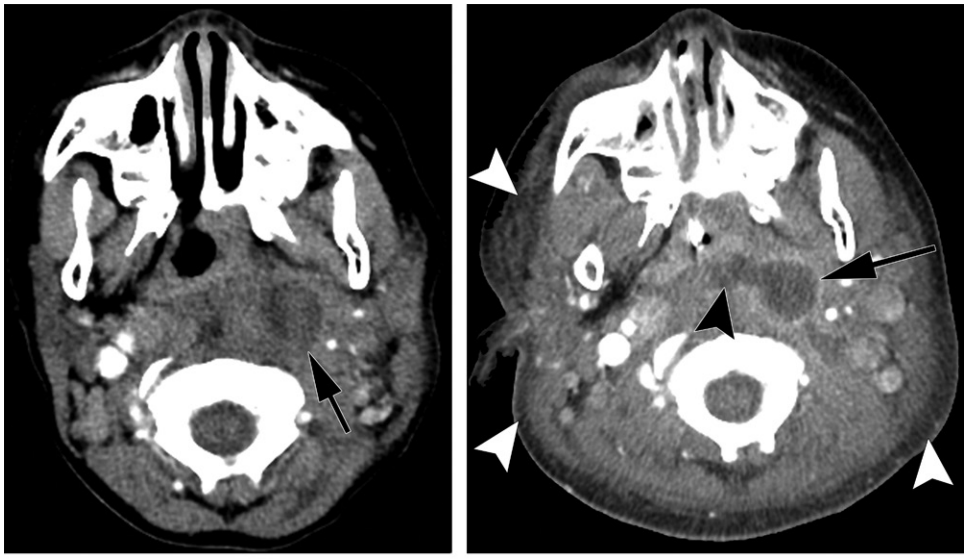

a. b.

Figure 5. Left retropharyngeal suppurated lymph node and retropharyngeal abscess in a 5-year-old boy. **(a)** Axial contrast-enhanced CT image shows a left retropharyngeal low-attenuation lymph node (arrow), consistent with internal suppuration. **(b)** Axial contrast-enhanced CT image obtained 3 days later, by which time the patient's condition had worsened such that intubation was required, shows that the suppurated lymph node (arrow) has ruptured into the retropharyngeal space (black arrowhead). Subcutaneous edema (white arrowheads) also is present.

is rare in adults. The adult cases that do occur usually are due to foreign body perforation (26).

In children, contrast-enhanced CT of the neck depicts suppurated lymph nodes as round structures posterior to the pharynx, with decreased internal attenuation and a rim of enhancement (Fig 5). A retropharyngeal abscess is a larger rim-enhancing collection that is not confined by the boundaries of the lymph node; rather, it extends across the retropharyngeal space (Fig 5) (24).

Retropharyngeal abscess must be differentiated from retropharyngeal edema, which may be an accessory finding due to other infectious processes or represent inflammation such as that due to prior radiation therapy or calcific tendinitis of the longus colli. Calcific tendinitis of the longus colli, technically a prevertebral process, results from an inflammatory reaction to hydroxyapatite deposits within the longus colli muscle or tendon (27). The CT diagnosis is dependent on the identification of abnormal calcific attenuation, which is usually seen within the longus colli tendon, inferior to the anterior arch of C1. Retropharyngeal edema involves the retropharyngeal space from side to side, with tapered superior and inferior ends; however, there is no rim enhancement (Fig 6) (24).

Angioedema refers to increased capillary permeability and extravasation of fluid that result in localized and transient edematous swelling of the skin or mucosa. Most cases are idiopathic; other cases involve hereditary, drug-related,

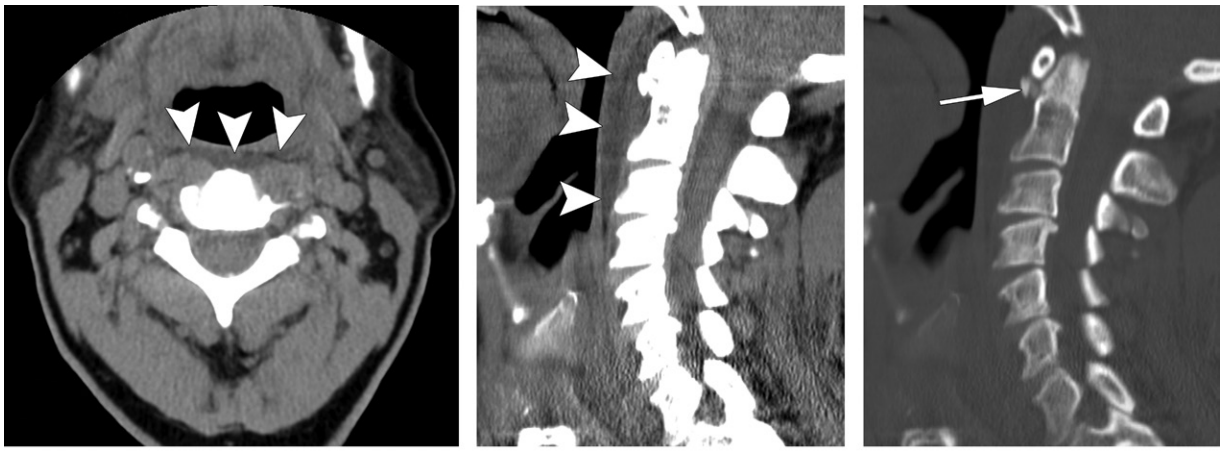

a. b. c.

Figure 6. Retropharyngeal edema due to calcific tendinitis of the longus colli in a 71-year-old woman. **(a, b)** Axial **(a)** and sagittal **(b)** nonenhanced CT images show retropharyngeal edema (arrowheads). Note the tapered superior and inferior margins in **b. (c)** Sagittal nonenhanced CT image (bone window) shows calcification (arrow) inferior to the anterior arch of C1, in the typical location for calcific tendinitis of the longus colli.

and/or allergy-related causes (28). The most commonly implicated drugs are angiotensin-converting enzyme inhibitors (either immediate or after months to years of taking the drug) and nonsteroidal anti-inflammatory agents (28). Manifestations may be minor conditions such as lip swelling or severe conditions such as laryngeal edema. Symptoms may develop over minutes to hours and resolve over 1–3 days.

The diagnosis of angioedema as the cause of head and neck swelling is usually based on clinical examination findings and the exclusion of other serious diagnoses. Therefore, neck CT may be performed to rule out treatable diagnoses. Neck CT images show focal or diffuse low-attenuation swelling of all or some of the soft tissues of the upper airway. For example, focal involvement may be seen in the tongue (Fig E5) (particularly in association with angiotensin-converting enzyme inhibitors), subcutaneous fat, lips (Fig 7), or soft palate, and it may be unilateral (28). Diffuse pharyngeal or laryngeal edema may be seen at CT, but it generally follows intubation, with the swollen soft tissues surrounding a previously placed endotracheal tube.

Evaluation for the presence of a foreign body is one of the few indications for which neck CT is performed without contrast material. In a large series (29), 76% of pharyngeal and esophageal foreign bodies were impacted just below the cricopharyngeus muscle, at approximately the C6 level. Also, fish bones (60% of cases) and chicken bones (16% of cases) were the most commonly retained foreign bodies in that series (29). Radiography may be unreliable, yielding false-positive and false-negative results. CT of the neck enables definitive identification and localization of potential foreign bodies. A bone will appear as a thin or flat radiopaque attenuating lesion lodged within the oropharynx, hypopharynx, or esophagus (Fig 8). Wooden foreign bodies have air attenuation in the acute phase and therefore are best detected by using lung windows, and they may mineralize and increase in attenuation with time (30). If there has been a perforation, extraluminal gas and fluid may be present. In this situation, repeat CT with intravenous contrast material may be necessary to delineate an abscess. A food bolus (commonly meat) in the esophagus will appear as a mixed-attenuation focus (Fig E6).

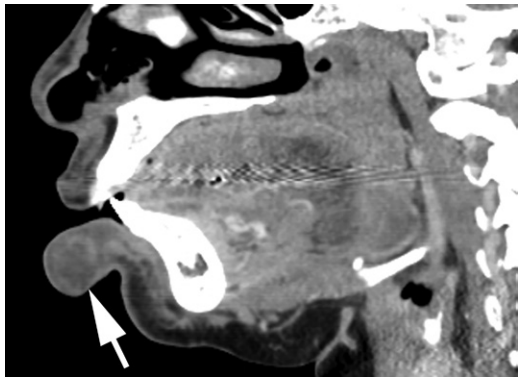

Figure 7. Sagittal contrast-enhanced CT image in a 45-year-old woman shows edema of the lower lip (arrow), consistent with angioedema.

Teeth and Periodontal Tissues

The teeth and surrounding structures are common culprits in cases of head and neck infection and are linked to systemic disorders such as cardiovascular disease (31,32). Infection may be localized to the tooth and its surrounding structures, or it may spread to distant locations. Primary causes of odontogenic infection include

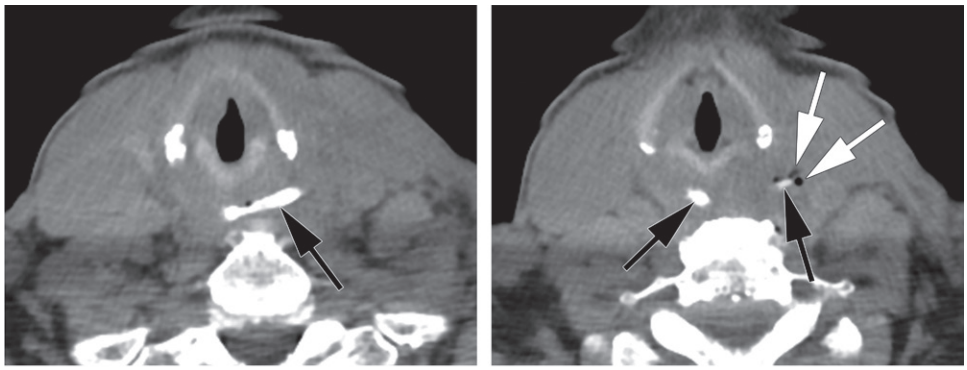

a. b.

Figure 8. Impacted chicken bone in a 78-year-old woman. Axial nonenhanced CT images show the radiodense bone (black arrows) in the cervical esophagus, posterior to the larynx. There is gas (white arrows in **b**) within the adjacent left lateral soft tissues, consistent with perforation. Rim enhancement cannot be assessed because contrast material was not administered.

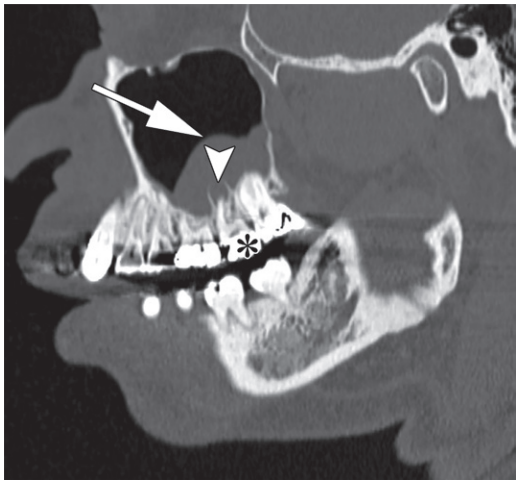

Figure 9. Odontogenic sinusitis in a 50-year-old man. Sagittal nonenhanced CT image shows a carious lesion in the second maxillary molar (*), obscured by streak artifact from dental amalgam. At the tooth apex, there is a periapical lucency and dehiscence of the bone plate (arrowhead) between the tooth and the maxillary sinus. There is associated adjacent polypoid mucosal disease within the maxillary sinus (arrow).

dental carious lesions, periodontal disease, and periapical disease. Dental caries appear on CT images as a defect or channel in the highly mineralized enamel of the tooth (Fig E7). When the caries are severe, large parts of the tooth crown or the entire crown may be absent. Tooth decay is a slow process and may be asymptomatic at first. When decay reaches the pulp chamber of the tooth, the pulp becomes infected, pressurized, ischemic, and ultimately necrotic. The infected material may be released at the apex of the tooth into the periapical region, causing periapical periodontitis, which may then develop into a periapical abscess, granuloma, or cyst. The development of osteomyelitis of the jaw is uncommon, unless there are other complicating factors such as prior radiation treatment or an open fracture.

Periodontal disease—that is, inflammation of the gingiva (gums)—can progress to periodontitis, in which the periodontal ligament that connects the tooth to the alveolar process, as well as the bone of the alveolar process, is lost (Fig E8). The last category of dental infection is pericoronitis, in which food material becomes trapped under a gum flap, commonly in the setting of a partially erupted third molar, and causes acute inflammation and infection (Fig E9). When reporting dental lesions, the amount of detail should be tailored to the given clinical setting. If the dental lesions are incidental and the extent of disease is limited, the lesions should be reported. If there is diffuse disease, a general statement should be made and may be followed by a description of the worst one or two lesions. If the dental disease is directly related to the reason that the examination was performed, a complete discussion is warranted.

Although the inflammatory process begins in or adjacent to a specific tooth, it may spread to nearby areas, including the orbits or intracranial compartment. For maxillary teeth whose roots abut the maxillary sinuses, a periapical inflammatory process may dehisce the bony separation between the tooth apex and the sinus and thereby cause odontogenic sinusitis. At CT, this condition appears as a soft-tissue–attenuation tract between the tooth apex and the sinus, with adjacent opacification of the sinus (Fig 9).

A periodontal abscess is a focal pocket of pus that forms adjacent to a tooth owing to the direct spread of infection, such as pericoronitis, or following a bony breakthrough of periapical disease into adjacent soft tissues. Bony breakthrough occurs at weak points of the alveolar process, which include the buccal surface throughout the maxilla and the lingual surface in the area of the mandibular molars. Infection may spread into the periodontal or more distant tissues as a result of

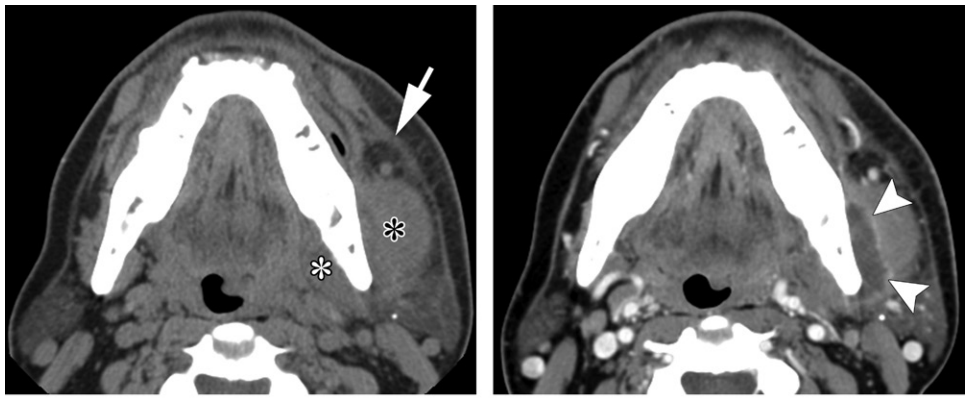

a. b.

Figure 10. Periodontal abscess in a 50-year-old man. **(a)** Axial nonenhanced CT image shows asymmetric soft-tissue thickening (white ∗) medial to the left mandibular ramus, as well as thickening of the left masseter muscle (black ∗). Owing to the lack of contrast enhancement, an abscess cannot be discerned. Note the thickening of the left platysma muscle (arrow). **(b)** Twelve hours later, the CT examination was repeated with intravenous contrast material administration, and the abscess (arrowheads) could be delineated between the mandibular ramus and masseter muscle.

dental procedures such as tooth extraction (33). If left untreated, there may be subsequent spread into adjacent muscle and deep spaces of the neck. To diagnose this condition, it is essential to administer intravenous contrast material to delineate the extent of disease and determine whether there is a drainable collection (Fig 10). There is typically a rim-enhancing hypoattenuating fluid collection adjacent to the involved tooth (Fig 10).

Ludwig angina is one of the most feared complications of dental infection. *Ludwig angina,* derived from the Latin word *angere,* meaning choke, refers to a polymicrobial infectious cellulitis involving the sublingual space above the mylohyoid muscle and the submandibular (ie, submylohyoid) space below the mylohyoid muscle. There is usually bilateral involvement, which may lead to airway obstruction at the level of the oral cavity and oropharynx (4). Ludwig angina manifests with fever, firm neck swelling, and difficulty swallowing or speaking (31). Most cases of Ludwig angina are related to dental infection (4) or recent extraction of the second or third molars, whose roots extend below the attachment of the mylohyoid muscle to the mandible (31). Regardless of whether the infection begins above or below the mylohyoid muscle or on the left or right side, it may spread around the free posterior edge of the mylohyoid muscle between these spaces and from left to right (34).

Oral piercings also may cause Ludwig angina (35). Infection spreads by means of contiguous extension and can lead to mediastinitis if left untreated. With Ludwig angina, CT images show inflammatory stranding and fluid in the submandibular and sublingual spaces, with or without abscesses or gas (Fig 11). As Ludwig angina is a "cellulitis," rim-enhancing components are not required to make the diagnosis. Lymphadenopathy is generally absent. The report should state the tooth of origin (when it can be determined), extent of infection, presence (or absence) of drainable collections, and degree of mass effect on the airway. Treatment consists of a combination of airway protection and antibiotics, and surgical drainage when necessary (4). When there are complications such as mediastinitis and mandibular osteomyelitis, these too must be addressed.

Thyroid Gland

The thyroid gland synthesizes the hormones triiodothyronine and thyroxine. At nonenhanced CT, the thyroid is hyperattenuating owing to its high iodine concentration. The thyroid normally enhances homogeneously following intravenous contrast material administration. Thyroid nodules are commonly encountered at neck imaging. Although a discussion of this topic, including characterization and workup, is beyond the scope of this review, this subject has been reviewed previously in this and other journals (36–38).

The reporting of thyroid enlargement should include a description of the extent of the enlargement and of any mass effect on the trachea, esophagus, and neck vessels (39). If there is tracheal compression, the craniocaudal length of the compression and the degree of reduction of the cross-sectional area should be estimated. The vocal cords should be evaluated for signs of asymmetry, as paralysis may occur owing to compression of the recurrent laryngeal nerve (40). The paralysis manifests as dilatation of the ipsilateral piriform sinus and laryngeal ventricle, medial rotation and thickening of the ipsilateral aryepiglottic fold, and anteromedial displacement of the ipsilateral arytenoid cartilage. Most cases

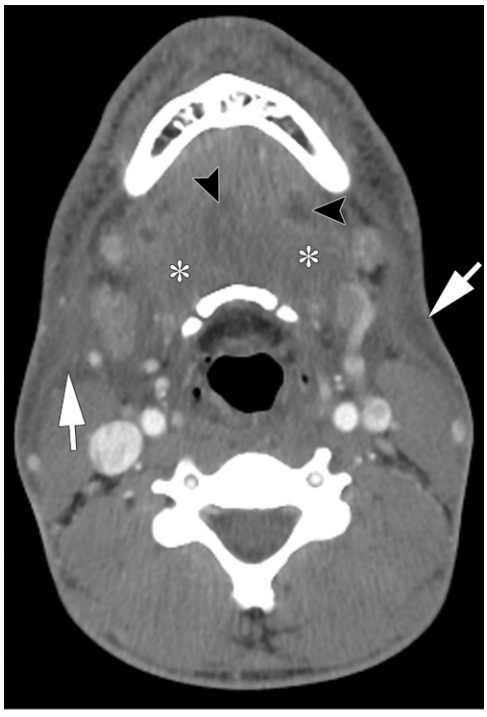

a.

b.

Figure 11. Ludwig angina in a 26-year-old man. Axial **(a)** and coronal **(b)** contrast-enhanced CT images show submandibular and sublingual edema (white ∗) with internal fluid pockets (arrowheads) consistent with pus. The oral cavity (black ∗ in **b**) is obliterated. Subcutaneous edema (arrows) also is present. When possible, specific involvement of the sublingual and submandibular spaces should be described owing to potential implications for drainage. However, owing to associated edema, as in this case, this may not always be possible.

of mediastinal extension are substernal, although a fraction of cases are posterior mediastinal. The degree of mediastinal extension, which is important when surgery is being planned, is measured from the sternal notch (39).

Graves disease is the most common autoimmune disease and the most common cause of hyperthyroidism. With this disease, autoantibodies stimulate the thyroid-stimulating hormone receptors on follicular cells, in effect mimicking thyroid-stimulating hormone. CT images show a diffusely enlarged and hyperenhancing gland (Fig 12). Thyroid gland infection is rare owing to the surrounding capsule, good vascularity, good lymphatic drainage, and internal iodine content (41). Still, risk factors for development of thyroid abscesses include immunodeficiency and underlying gland abnormalities such as thyroid nodules, thyroid cancer, and fourth branchial cleft anomalies. Fourth branchial cleft fistulas or sinus tracts, which are usually on the left, begin at the apex of the piriform sinus and descend along the tracheoesophageal groove to the cranial portion of the thyroid gland, and they may lead to recurrent infection (12).

Goiter refers to enlargement of the thyroid gland. Iodine deficiency is an important cause of goiter worldwide, but it is uncommon in the United States. In the United States, the most common cause of goiter is Hashimoto thyroiditis, whereby the gland is unable to produce an adequate amount of thyroid hormone and is continuously stimulated by thyroid-stimulating hormone to enlarge. Other causes of goiter include Graves disease and toxic or nontoxic nodular goiter. Factors that predispose individuals to having nodular goiter include iodine deficiency and genetics; the exact causal mechanism is uncertain. Nodular goiter usually begins as diffuse gland enlargement and progresses to the nodular form. On CT images, goiter appears as an enlarged nodular heterogeneous gland with regions of hemorrhage, cysts, necrosis, and calcification (Fig 13). The enlargement may be asymmetric (39).

The two superior parathyroid glands are most commonly located dorsal to the superior poles of the thyroid gland, and the two inferior parathyroid glands are most commonly located inferior, dorsal, or lateral to the inferior thyroid pole (42). They measure up to 5 mm in diameter and, owing to their small size, generally are not well seen at routine CT of the neck (42). When these glands are enlarged owing to hyperplasia or adenoma, they may be detected at CT. Therefore, when a parathyroid gland is identified and the patient has an elevated serum calcium level, it is prudent to recommend endocrine evaluation to determine whether parathyroid disease is the underlying cause.

Salivary Glands

The major salivary glands include the parotid, submandibular, and sublingual glands. At CT, the attenuation of the parotid gland in adults is usually intermediate, between the attenuation of fat and that of muscle, owing to its fat content. In children and some adults, the parotid gland

is isoattenuating to muscle. Intraparotid ducts typically are not visible unless they are dilated. The parotid gland is the only salivary gland that contains lymph nodes. Accessory parotid tissue often can be seen along the course of its duct (Stensen duct) superficial to the masseter muscle. The submandibular and sublingual glands have higher attenuation than does the parotid gland owing to their lower fat content.

Sialadenitis refers to inflammation of a salivary gland. The populations that are most at risk for acute sialadenitis are elderly persons and neonates. Acute unilateral sialadenitis most commonly involves the parotid gland and is usually caused by an ascending bacterial infection from the oral cavity in the setting of salivary stasis and dehydration (25). *Staphylococcus aureus* is the most common infecting organism (43). Sialolithiasis with an obstructing ductal stone is an important cause of submandibular sialadenitis; 80%–90% of sialoliths occur in the submandibular glands, while 10%–20% occur in the parotid glands. The higher rate of stone formation in the submandibular gland is due to the small papillary orifice, ascending course of the (Wharton) duct, higher viscosity of saliva, and slow salivary flow rate (25). Causes of bilateral sialadenitis include viral infection, radiation, immunoglobulin G4–related sialadenitis (of the submandibular glands), and Sjögren syndrome (of the parotid glands). Viral sialadenitis, most commonly mumps, typically (in 85% of cases) occurs in children younger than 15 years and is bilateral in 90% of cases (44). Ninety percent of cases of viral sialadenitis involve the parotid glands, while 10% also involve the submandibular glands (44).

In the acute phase, sialadenitis manifests at contrast-enhanced CT as enlargement and heterogeneous hyperenhancement of the affected gland(s), with surrounding fat stranding (Fig 14). If there is an obstructing ductal stone (Fig 14), ductal dilatation also is present. The involved glands and their ducts should be inspected for stones. However, occasionally this may be difficult because these structures are obscured by streak artifact from dental amalgam. Bacterial sialadenitis may be complicated by the formation of a rim-enhancing abscess or multiple small abscesses.

Lymph Nodes

Adenopathy in the neck can be caused by many different entities, including infection, inflammatory disease, and malignancy. Although acute conditions are the first that come to mind, malignancy must remain in the differential diagnosis. Normal lymph nodes demonstrate an ovoid morphology, a fatty hilum, smooth margins, and homogeneous isoattenuation to muscle at CT. Cervical lymph nodes can be classified into levels (I–VII) and anatomic groups (supraclavicular, parotid, retropharyngeal, and occipital stations) according to established criteria (45).

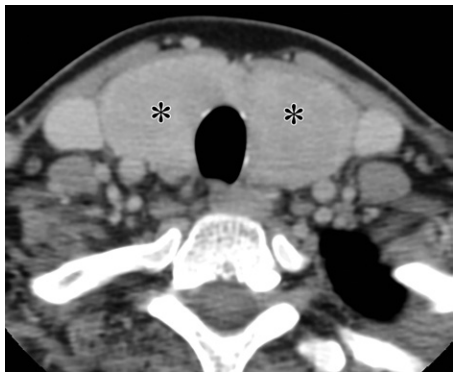

Figure 12. Graves disease in a 29-year-old woman. Axial contrast-enhanced CT image shows a homogeneously enlarged thyroid gland (*).

Figure 13. Thyroid goiter in a 56-year-old woman. Axial nonenhanced CT image shows an enlarged thyroid gland (black *) surrounding the trachea (arrow), which is narrowed to 8 × 5 mm. Internal cysts and a calcification also are noted. In addition, there is an indeterminate low-attenuation nodule or complex cyst (white *) in the isthmus.

Viral infections are the most common cause of reactive adenopathy in children and young adults. CT reveals mildly enlarged and enhancing nodes without surrounding fat stranding. Bacterial infections typically cause more prominent nodal enlargement and also cause surrounding inflammatory change. In children, lymph nodes may suppurate, and these nodes become centrally hypoattenuating with peripheral enhancement (46).

Mycobacterial cervical lymphadenitis, referred to as scrofula, may be tuberculous or nontuberculous (47). Seventy-five percent of the time, scrofula is unilateral. In the acute phase, the lymph nodes are enlarged and homogeneously enhance at CT. As caseation occurs, the nodes become

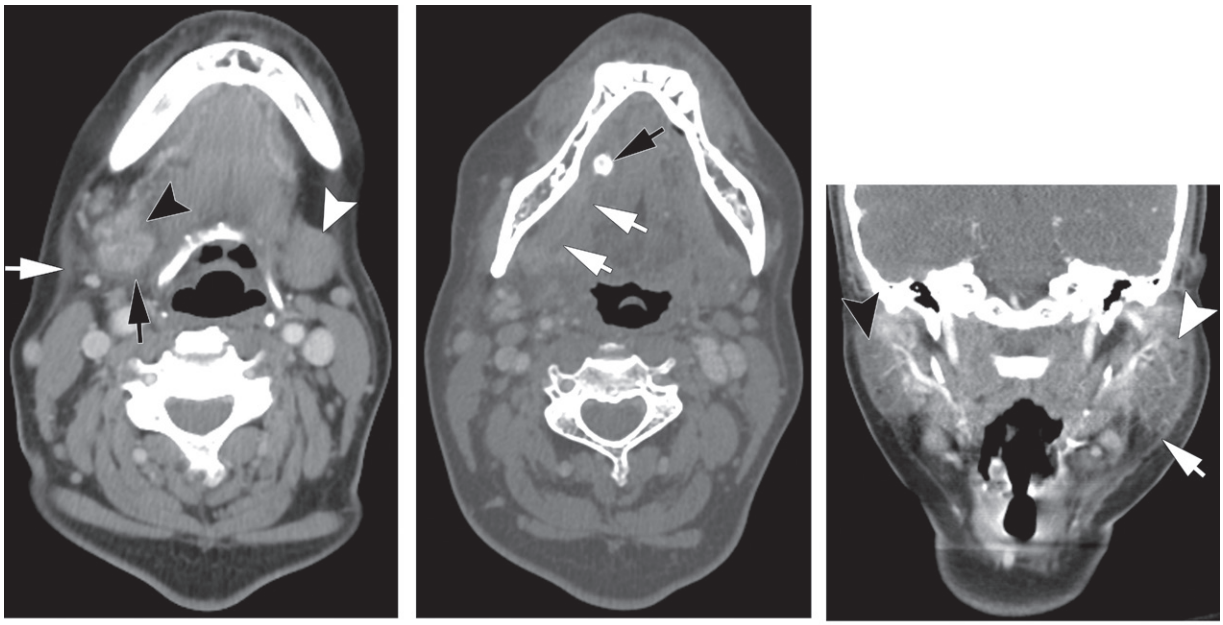

a. b. c.

Figure 14. Sialadenitis in two patients. **(a, b)** Acute right submandibular sialadenitis in a 57-year-old woman. Axial contrast-enhanced CT image **(a)** shows an enlarged hyperenhancing right submandibular gland (black arrowhead) with internal and surrounding edema (black arrow) and overlying thickening of the platysma muscle (white arrow). In comparison, the left submandibular gland (white arrowhead) is normal. Axial contrast-enhanced CT image **(b)** obtained superior to **a** shows a stone (black arrow) in the distal portion of the dilated right submandibular duct (white arrows). **(c)** Coronal contrast-enhanced CT image at the level of the parotid glands in a 22-year-old woman with acute left parotiditis shows edema, enlargement, and hyperenhancement of the left parotid gland (white arrowhead). There is also thickening of the left platysma muscle (arrow). In comparison, the right parotid gland (black arrowhead) is normal. Additional images (not shown) did not show a stone within or along the course of the parotid duct.

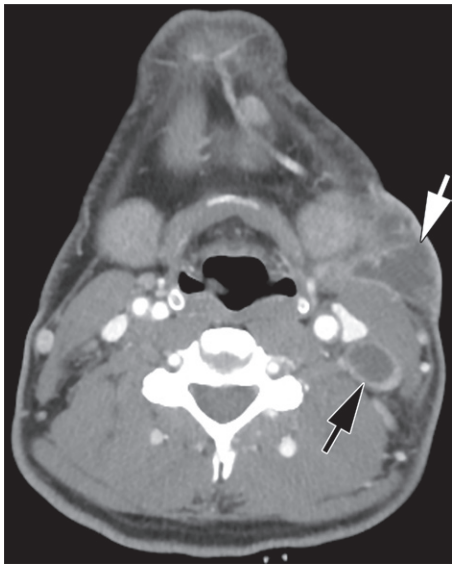

Figure 15. Mycobacterial lymphadenitis (scrofula) in the left side of the neck in a 43-year-old man. Axial contrast-enhanced CT image shows a centrally hypoattenuating cystic lymph node (black arrow) with minimal surrounding fat stranding. Another lymph node (white arrow) has ruptured and fistulized to the skin.

centrally hypoattenuating and cystic, with perinodal fat stranding that is milder than what is seen with bacterial adenitis (Fig 15). If the capsules of individual lymph nodes rupture, they may coalesce into a single nodal mass (47). Fistulization and drainage to the skin also may occur (Fig 15).

A comprehensive discussion of malignant lymphadenopathy is beyond the scope of this article and has been reviewed elsewhere (14,48). However, a few points should be made to differentiate malignant adenopathy from infectious adenopathy. Nodal metastasis is a common feature of squamous cell carcinoma of the head and neck. At CT, these nodes are enlarged, rounder than the normally elongated cervical nodes, and centrally necrotic. Nodal metastases usually lack the surrounding inflammatory stranding that is seen with bacterial adenitis. However, extracapsular tumor extension can mimic inflammatory stranding where there are indistinct nodal margins or after biopsy and radiation when the lymph node may have poorly defined margins (45). In keeping with lymphatic drainage patterns, the location of a nodal metastasis can suggest the site of a primary head and neck malignancy. Cervical lymph node involvement is the most common manifestation of Hodgkin disease involving the head and neck (48). Disease may be unilateral or bilateral, with enlarged lymph nodes or a confluent soft-tissue mass (48). In contrast to squamous cell carcinoma–related adenopathy, central necrosis is an uncommon feature of lymphoma (48). As a last point, either clinical or imaging

follow-up or tissue sampling may be necessary to make a definitive diagnosis.

Vascular Structures

The common carotid, internal carotid, and vertebral arteries traverse the neck and can be readily evaluated at standard contrast-enhanced neck CT. While dedicated CT angiography is generally superior for the specific evaluation of arterial disease, many arterial abnormalities can be identified on standard soft-tissue neck CT images. Therefore, the carotid and vertebral arteries should be traced at every neck CT examination. Normally, the walls of the carotid and vertebral arteries have a smooth contour along their external and luminal surfaces and are uniform in thickness, measuring 1–2 mm (49). The arterial lumens generally are uniform in diameter, except in the carotid bulb, a region of normal luminal widening at the origin of the internal carotid artery. The vertebral arteries course along the posterior neck, passing through the transverse foramina of the C2–C6 vertebrae.

Atherosclerosis of the cervical arteries, particularly at the carotid bulbs, is extremely common in middle-aged and older adults and can be evaluated by using multiple modalities, including CT (50). Arterial dissection is characterized by a defect in the intimal layer of the artery that allows passage of blood into the arterial wall. This defect leads to the formation of a false lumen, which is frequently accompanied by narrowing or occlusion of the true lumen (51).

Although primary vascular inflammation is a relatively rare cause of neck pain, it is occasionally identified at neck CT. Cervical arterial inflammation may reflect a systemic large-vessel vasculitis such as Takayasu arteritis. In this setting, extensive arterial wall thickening may be seen and usually also involves the visualized mediastinal arteries (Fig E10). In contrast, carotidynia is a poorly understood idiopathic condition characterized by neck pain and focal tenderness in the region of the carotid bifurcation. Associated imaging abnormalities may include mural thickening of the affected carotid artery and stranding of surrounding fat (Fig 16) (52).

Portions of the circle of Willis are typically included at CT examinations of the neck, and consequently, intracranial arterial abnormalities may be visualized. An intracranial aneurysm is a particularly important finding that may be incidentally encountered at neck CT. The prevalence of intracranial aneurysm in the general population without comorbidities has been estimated to be 3.2% (53). Owing to the risk of aneurysmal rupture with devastating subarachnoid hemorrhage and the availability of effective treatment options, the intracranial arteries should be scrutinized in every case.

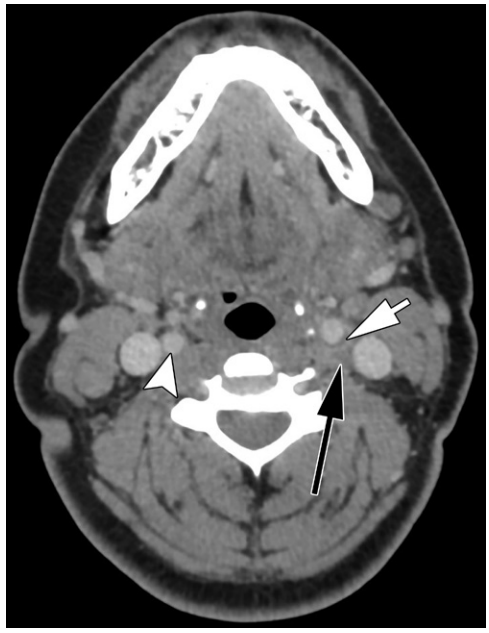

Figure 16. Carotidynia in a 29-year-old woman. Axial contrast-enhanced CT image shows pericarotid infiltration (black arrow). A soft plaque (white arrow) causing mild luminal narrowing also is present at the carotid bulb, with possible enhancement of the adjacent vessel wall. In comparison, the right internal carotid artery (arrowhead) is normal.

Numerous veins are visible on contrast-enhanced neck CT images. The largest and most important veins are the internal jugular veins, which arise from the intracranial dural venous sinuses and extend to the mediastinum. Normal internal jugular veins are frequently asymmetric in caliber. Valves, which are visible in the internal jugular veins occasionally, and heterogeneous enhancement due to the mixing of opacified and nonopacified blood should not be mistaken for thrombosis.

Jugular thrombosis may be complete, in which case the vein is nonopacified and usually enlarged (when acute), or partial, in which case a sharply marginated filling defect is seen. Edema of adjacent fat planes may be present. At nonenhanced CT, there may be abnormally increased attenuation in the thrombosed vein. The thrombus may extend superiorly to the sigmoid sinuses or inferiorly to the mediastinal veins. Additional imaging of the head or chest may be necessary to completely visualize the clot.

A jugular venous thrombus may be bland, tumorous, or septic. Bland thrombus is frequently associated with indwelling venous catheters, such as hemodialysis catheters, and can also be seen in thrombophilic conditions. In Lemierre syndrome, septic thrombophlebitis of the internal jugular vein

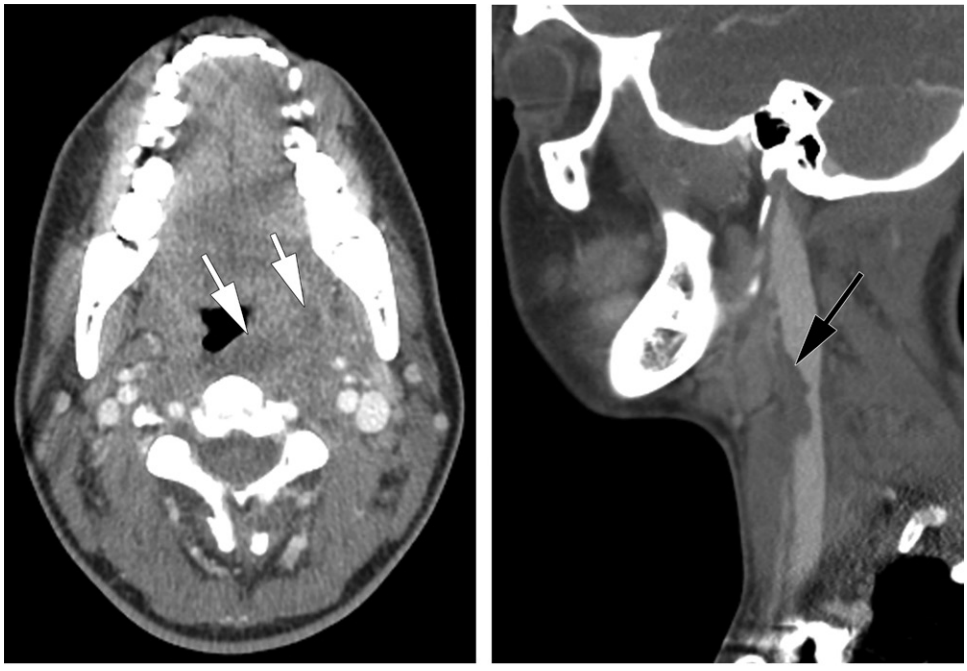

a. b.

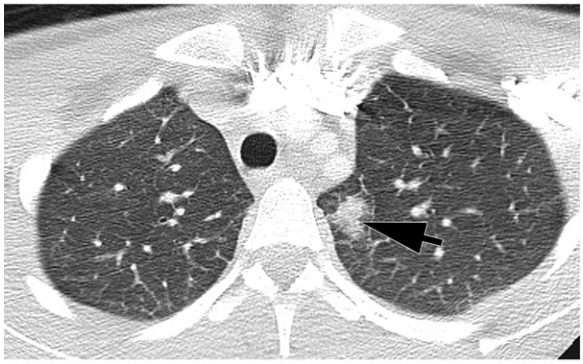

c.

Figure 17. Lemierre syndrome in a 15-year-old girl. **(a)** Axial contrast-enhanced CT image shows left peritonsillar edema (arrows), consistent with tonsillitis. **(b)** Sagittal contrast-enhanced CT image shows a clot (arrow) in the left internal jugular vein. **(c)** Axial contrast-enhanced CT image (lung window) obtained inferior to **a** shows a nodular opacity (arrow) at the left lung apex, consistent with a septic pulmonary embolus. Additional similar lesions were seen on other images (not shown).

occurs secondary to a pharyngeal infection such as pharyngitis or PTA (Fig 17). Associated septic pulmonary emboli are frequently present. Systemic dissemination of infection may occur, particularly if treatment is delayed, and is associated with significant mortality, even with antimicrobial treatment (54). Therefore, identification of a peritonsillar or retropharyngeal abscess should prompt a reflex search for a jugular venous thrombus and septic pulmonary emboli in the included lung apices.

Bony Airspaces

The pneumatized spaces of the head and neck include the paranasal sinuses, which communicate with the nasal cavity, and the mastoid air cells, which communicate with the tympanic (middle ear) cavity. The paranasal sinuses consist of the maxillary, sphenoid, and frontal sinuses, as well as the ethmoid air cells. The mastoid air cells lie predominantly within the mastoid portion of the temporal bone but vary in extent considerably between individuals. In some people, pneumatized spaces extend to the apical (medial) portion of the temporal bone and are termed *petrous apex air cells.* The normally aerated paranasal sinuses and mastoid air cells have an imperceptibly thin mucosal lining.

Sinusitis may be acute or chronic and have an allergy-related, viral, bacterial, or fungal cause. Most patients with acute sinusitis do not require imaging. However, if there is concern regarding a possible alternative diagnosis or spread to the orbits or brain, contrast-enhanced maxillofacial or neck CT is indicated (26). At CT, acute bacterial sinusitis is characterized by the presence of fluid and mucosal thickening in one or more sinuses (55). Fluid within the sinus may layer dependently, resulting in an air-fluid level, or it may have a frothy (bubbly) appearance.

It is important to note that the presence of intrasinus fluid or mucosal thickening is not specific for acute sinusitis and may also be seen, for example, in the setting of upper respiratory

tract infection or nasogastric tube placement. Forty-four percent of adults and 50% of children have imaging findings of sinusitis, although they undergo imaging for other reasons (56). Furthermore, mucosal thickening can persist for 8 weeks following the resolution of sinusitis (56). Therefore, for the diagnosis of acute sinusitis, supporting clinical signs and symptoms such as fever and pain overlying the affected sinuses must be present.

Complications of acute bacterial sinusitis include extension into the orbit with development of a subperiosteal abscess and orbital cellulitis; extension into the overlying soft tissues (eg, Pott puffy tumor); and intracranial extension with development of an epidural abscess, subdural empyema, or cerebritis with or without brain abscess. Cavernous sinus thrombosis is seen occasionally. These complications are discussed in greater detail in the following sections.

Fungal sinus disease includes allergic fungal sinusitis and invasive fungal sinusitis. Allergic fungal sinusitis is a chronic inflammatory condition that is characterized at CT by extensive opacification of multiple sinuses, which are typically expanded. Hyperattenuating material, reflecting allergic mucin, is frequently seen in the affected sinuses. Acute invasive fungal sinusitis typically occurs in immunocompromised patients and can be rapidly progressive and life-threatening (57). Zygomycetes fungi such as *Mucor* species cause up to 80% of cases in patients with diabetes, while *Aspergillus* species cause up to 80% of cases in patients with neutropenia—for example, in cases of chemotherapy, bone marrow transplant, and acquired immunodeficiency syndrome (57). Acute invasive fungal sinusitis is characterized by unilateral destruction of the osseous margins of the sinus, with extension into adjacent structures such as the orbits, intracranial compartment, and subcutaneous tissues. It is important to note that due to the angioinvasive nature of this process, extension to adjacent structures may occur even with intact bony sinus walls and minimal mucosal thickening (57).

Infiltration of the periantral fat is a classic finding of acute invasive fungal sinusitis (Fig 18) (58). A chronic form of invasive fungal sinusitis may occur in immunocompetent patients, in whom the condition progresses over months to years (57). A masslike hyperattenuating focus is typically seen in a sinus or multiple sinuses, and there is gradual sinus wall destruction. Involvement of the periantral fat, orbits, or intracranial compartment indicates invasion (57). As a final note regarding this disease, when fungal sinusitis is suspected, this should be mentioned in the report, as the pathologist can use special stains, such as silver and periodic acid–Schiff stains, to highlight organisms that have invaded the vessel walls and lumen (59).

Figure 18. *Mucor* sinusitis in a 59-year-old woman with diabetes. Axial contrast-enhanced CT image shows an air-fluid level (confirmed on other images, not shown) in the left maxillary sinus (*), consistent with sinusitis. Classic periantral fat stranding (black arrow) is seen on the left, as compared with the normal periantral fat (white arrow) on the right. The findings in this case show that minimal sinus opacification does not exclude the diagnosis of invasive fungal sinusitis.

Acute otomastoiditis predominantly affects children, and it occurs when otitis media spreads to involve the mastoid air cells. Uncomplicated otomastoiditis manifests at CT as opacification of the middle ear cavity and mastoid air cells, without osseous destruction. Although the presence of mastoid air cell fluid is common, it does not necessarily indicate mastoiditis. The presence of supportive clinical features, such as tenderness over the mastoid prominence of the temporal bone, is required for diagnosis.

As mastoiditis progresses, the mastoid septa become eroded. The condition involving mastoid effusion in conjunction with septal erosion is referred to as coalescent mastoiditis (60). Comparing the side of the clinical symptoms with the contralateral side can be helpful in determining whether there is erosion of the mastoid septa. Complications of mastoiditis include erosion of the outer cortex of the mastoid bone with development of a neck abscess (ie, Bezold abscess) (Fig 19), as well as erosion of the inner cortex of the mastoid bone, which can lead to sigmoid sinus thrombosis, epidural abscess, or cerebritis with or without brain abscess (60). MRI is useful for evaluating intracranial extension of mastoiditis.

In patients with pneumatized petrous apices, petrous apicitis, a condition analogous to mastoiditis, can develop in the petrous apex (61). Infection typically spreads from the tympanic cavity

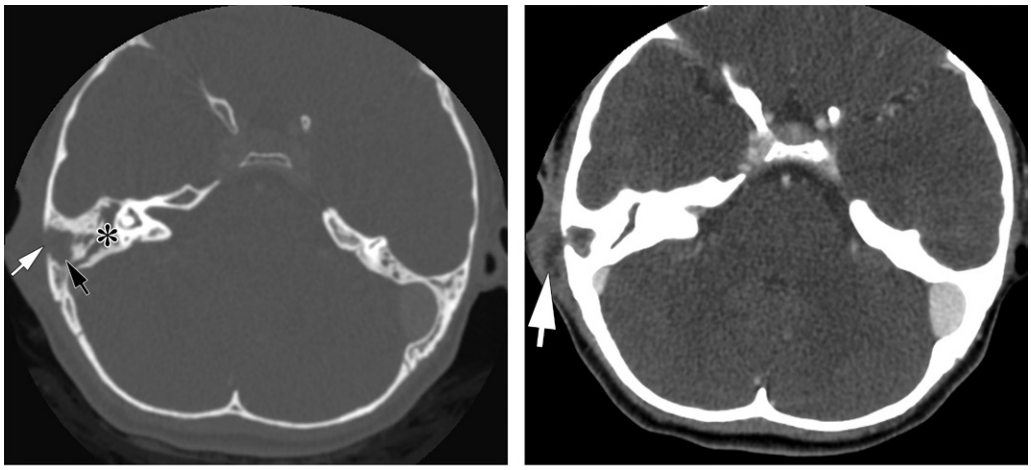

a. b.

Figure 19. Right coalescent mastoiditis with extracranial abscess in a 13-year-old girl. **(a)** Axial contrast-enhanced CT image (bone window) shows tympanomastoid opacification (*). There is coalescence of the right mastoid air cells (black arrow) with breakthrough of the overlying cortex (white arrow). **(b)** Image in **a** obtained in soft-tissue windows shows an overlying or developing abscess (arrow).

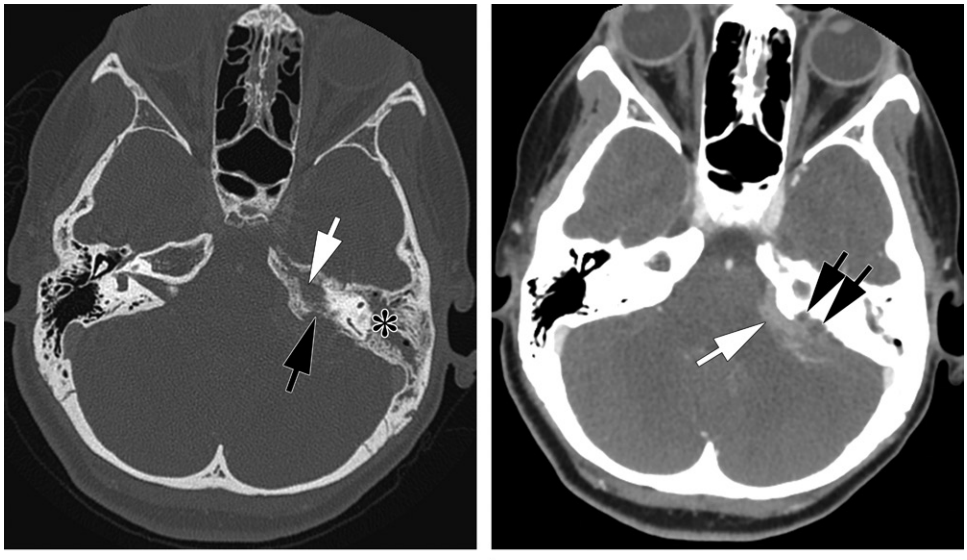

a. b.

Figure 20. Left petrous apicitis in an 11-year-old girl who presented with ear drainage and diplopia. **(a)** Axial contrast-enhanced CT image (bone window) shows left tympanomastoid opacification (*), as well as opacification and coalescence of air cells at the petrous apex (white arrow). There is also bone dehiscence (black arrow) along the dorsal aspect of the petrous apex. **(b)** Image in **a** obtained in soft-tissue windows shows epidural phlegmon (white arrow) and nonenhanced foci (black arrows), consistent with abscess.

to the air cells in the petrous apex, and it may lead to osseous erosion and subsequent involvement of adjacent skull base structures. Gradenigo syndrome is a classic manifestation of petrous apicitis and constitutes the triad of facial pain (reflecting involvement of the trigeminal nerve in Meckel's cave), ophthalmoplegia (reflecting involvement of the sixth cranial nerve in Dorello's canal), and otalgia and otorrhea (reflecting otomastoiditis).

With petrous apicitis, CT images show opacification of the petrous apex air cells, which may also demonstrate coalescence, with more extensive erosion of the petrous apex in advanced cases (Fig 20). The intracranial extension may result in cavernous sinus or sigmoid sinus venous thrombosis, epidural abscess, subdural empyema, meningitis, or cerebritis with or without brain abscess. MRI should be performed when intracranial extension is suspected.

Cervical Spine

At standard CT evaluation of the neck, the craniocervical junction and the entire cervical spine are included, and abnormalities of the cervical spine are commonly seen. In the setting of suspected cervical spine disease, dedicated CT or MRI of

the spine is preferred over neck CT. However, the symptoms of cervical spine disease may mimic those of extraspinal entities, prompting the use of neck CT with a soft-tissue protocol. Therefore, in the acute setting, careful inspection of the cervical spine is mandatory at neck CT.

Bacterial infection of an intervertebral disk, or discitis, is typically accompanied by infection of the adjoining vertebrae (osteomyelitis) and may be due to hematogenous seeding, direct spread from retropharyngeal or paraspinal infection, or inoculation by way of spinal instrumentation. CT findings of bacterial discitis and osteomyelitis include loss of disk space height and erosion of the adjacent vertebral endplates (62). Inflammatory changes of the paraspinal soft tissues also are usually present and include obscuration of paraspinal fat planes, paraspinal abscesses, and retropharyngeal edema (Fig E11). Eventually, severe bone destruction and deformity can develop. Noninfectious processes occasionally mimic the findings of discitis and osteomyelitis and should be considered if paraspinal inflammatory changes or abscesses are absent (63). MRI is superior to CT for the diagnosis of discitis and osteomyelitis, particularly early in the course of disease, and should be performed if discitis or osteomyelitis is suspected.

Infection of the spinal facet (zygapophyseal) joints is an uncommon cause of neck pain. In this condition, CT may demonstrate irregularity and erosion of the articular bone, fluid in and around the joint, and/or infiltration of adjacent paraspinal fat planes. Infectious involvement of the epidural space may occur in isolation or within the context of vertebral infection. Visualization of the spinal canal is quite limited with CT, even with administration of contrast material. However, one can often distinguish the lower-attenuation cerebrospinal fluid from the higher-attenuation spinal cord with use of narrow window settings, and it may be possible to identify an abnormal peripheral (epidural) area of attenuation adjacent to evidence of discitis or septic arthritis (Fig 21).

Degenerative disease of the cervical spine is commonly seen at neck CT and frequently incidental. However, in the setting of neck pain, degenerative disease may be relevant with regard to the symptoms reported by the patient. The presence of degenerative changes should be noted, at least in general terms, and if severe spinal canal stenosis or an alignment abnormality is present, a more detailed description is warranted. Anterior spinal osteophytes are frequently seen in the setting of degenerative disease and are usually asymptomatic. However, large anterior osteophytes, as seen in the setting of diffuse idiopathic skeletal hyperostosis, can cause dysphagia owing to compression of the esophagus (64).

Figure 21. Epidural phlegmon in a 59-year-old man with human immunodeficiency virus infection and a history of intravenous drug use. Sagittal contrast-enhanced CT image shows prevertebral edema (*). There is also thin enhancing material in the anterior epidural space extending from the C1–C5 vertebrae (arrows), consistent with epidural phlegmon. Surgical drainage was performed.

Orbits and Imaged Brain

The orbits are included in all CT examinations of the neck. The reader is referred to the relatively recent article regarding orbital emergencies published in this journal (65).

Progression of intraorbital infection can result in thrombosis of the superior ophthalmic vein, which can then propagate to the cavernous sinus. Superior ophthalmic vein thrombosis appears on contrast-enhanced CT images as enlargement of the superior ophthalmic vein, with a central filling defect, and surrounding fat stranding. When cavernous sinus thrombosis occurs, there is outward bulging of the normally straight or concave lateral wall of the cavernous sinus, with filling defects in the sinus that correspond to clots (66). If the superior ophthalmic vein is not thrombosed, it becomes enlarged owing to impaired drainage into the cavernous sinus (Fig 22).

Infection involving the orbits, paranasal sinuses, or temporal bones can spread to the intracranial compartment by means of bone dehiscence or through valveless diploic veins. While intracranial extension is often clearly visible on contrast-enhanced CT images, once

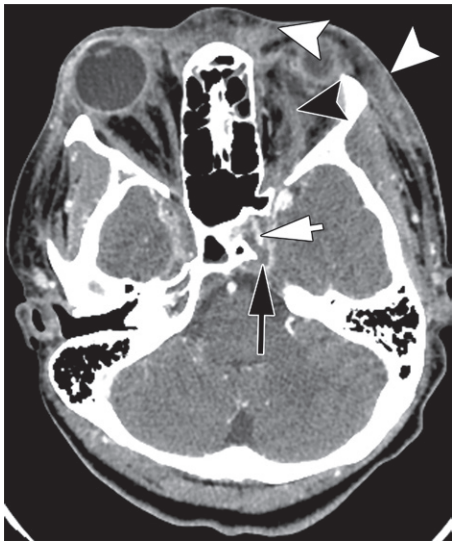

Figure 22. Cavernous sinus thrombosis in a 14-year-old girl. Axial contrast-enhanced CT image shows incomplete enhancement of the left cavernous sinus (black arrow), through which the enhancing internal carotid artery (white arrow) is coursing. The left superior ophthalmic vein (black arrowhead) is dilated and not enhanced. There is associated subcutaneous edema (white arrowheads) of the face and edema in the left orbit.

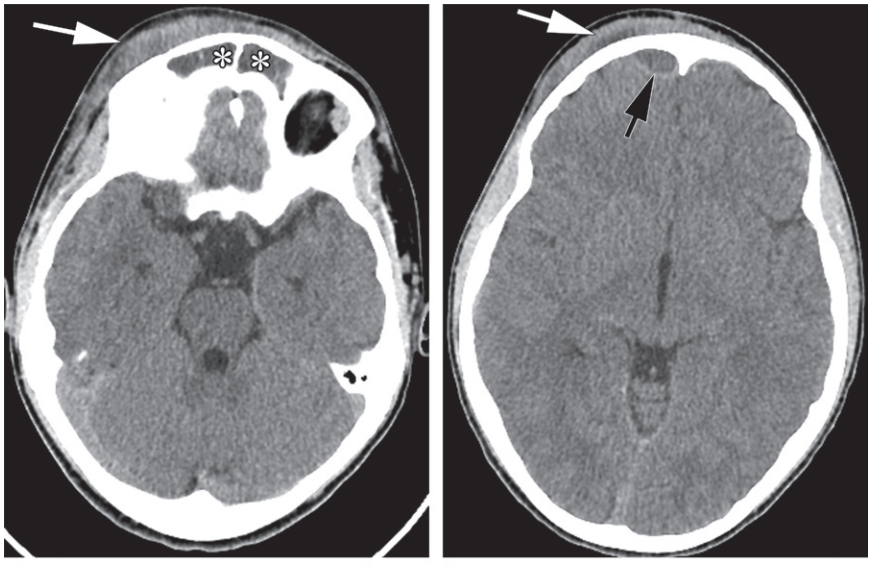

Figure 23. Epidural abscess and subgaleal phlegmon in a 13-year-old boy. Axial contrast-enhanced CT images show opacification of the frontal sinuses (* in **a**) and a rim-enhancing epidural fluid collection (black arrow in **b**) just superior to the frontal sinus, which is consistent with an epidural abscess. There is also enhancing subgaleal soft tissue (white arrow), consistent with phlegmon.

there is concern regarding possible intracranial extension of infection, contrast-enhanced MRI should be performed, as it is more sensitive and can facilitate better delineation of the extent of disease. In addition, there should be a low threshold for MRI when an invasive fungal infection is suspected in an immunocompromised patient, as long as imaging does not cause a delay in performing a potentially life-saving surgical intervention (67).

Epidural abscesses are collections of pus in the epidural space and are most commonly due to sinus infections (68). CT images show a rim-enhancing collection with characteristics of an epidural collection (eg, lentiform in shape, usually not crossing sutures) (Fig 23). When these abscesses result from a temporal bone infection such as mastoiditis, a rim-enhancing epidural collection may be seen between the mastoid bone and the cerebellum or temporal lobe (Fig 20). Subdural empyemas, like epidural abscesses, are often secondary to sinusitis or mastoiditis and appear as rim-enhancing collections or confluent enhancement in the subdural space. Ultimately, infection in the meninges can extend to involve the brain parenchyma, with cerebritis appearing on CT images as an area of low attenuation adjacent to sinus or mastoid infection. A brain abscess appears as an intraparenchymal hyperattenuating ring that enhances after contrast material administration, with the internal and surrounding hypoattenuating areas representing purulent material and edema, respectively (Fig 24).

In addition to evaluating for intracranial extension of infection, one must also scrutinize the imaged brain for incidental findings. On a typical neck CT image, a substantial portion of the inferior frontal and temporal lobes, along with the

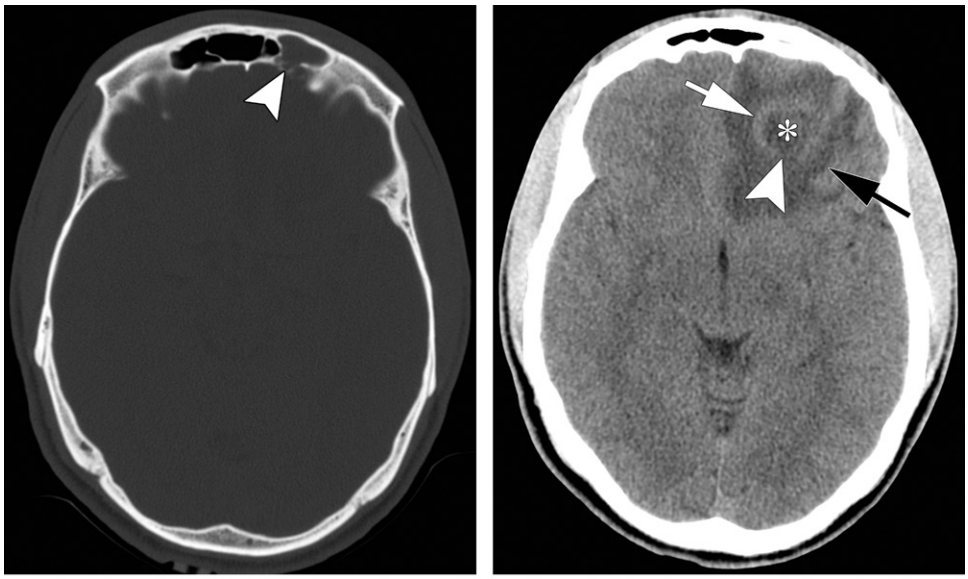

a. b.

Figure 24. Left frontal sinusitis and left frontal lobe abscess in a 22-year-old man. **(a)** Axial nonenhanced CT image (bone window) shows an opacified left frontal sinus, with thinning of the posterior wall of the sinus (arrowhead). **(b)** Axial nonenhanced CT image obtained just superior to **a** shows an abscess with a low-attenuation center (*), a thicker abscess rim (white arrow), and surrounding edema (black arrow). Typical thinning of the abscess capsule (arrowhead) is present on the side facing the ventricle. These findings were confirmed at contrast-enhanced MRI (not shown). Culture analysis revealed α-hemolytic *Streptococcus* as the causative organism.

brainstem, posterior fossa, and suprasellar cistern, which includes the circle of Willis, is visible. Intracranial masses, large aneurysms of the circle of Willis, acute infarcts, and intracranial hemorrhages are additional examples of intracranial anomalies that can be seen on neck CT images.

Lung Apices

The lung apices are visible on all CT scans of the neck. Visible structures include the upper lobe lung parenchyma and pleural surfaces, as well as the upper lobe pulmonary arteries, veins, and airways. Numerous common and clinically significant pathologic conditions may be seen in the lung apices at neck CT. Although many of these conditions are identified incidentally, recognizing them can still be vital for patient management.

Pneumonia appears as nodular and/or consolidative opacities in the lung parenchyma. CT is more sensitive than chest radiography for detection of pneumonia. As such, it is possible that pneumonia that was not appreciated on a previously obtained chest radiograph may be visible in the lung apices on a neck CT image. It is also possible that perceived opacities in the lung apices seen on a chest radiograph may not be present on a subsequently obtained CT image (69). Given the limitations of chest radiography in the diagnosis of pneumonia, one must take advantage of any opportunity to scrutinize a portion of the lungs with a more sensitive imaging modality.

Nodules or masses are frequently encountered on CT images, and the detection of them in the lung apices at neck CT can be helpful for the analysis of other examination findings. For example, identification of nodules representing septic emboli in the presence of internal jugular vein thrombosis can confirm the diagnosis of Lemierre syndrome (discussed earlier). The presence of metastases in the lung apices can aid in characterizing nonspecific neck CT findings as likely neoplastic rather than infectious or inflammatory. Incidentally detected nodules or masses may also represent previously unknown lung malignancy. Study findings have shown that a significant proportion of lung cancers missed at chest radiography are in the upper regions of the lung (70). When they are detected, appropriate follow-up should be recommended and communicated.

Finally, important information regarding the fluid status of the patient can be gleaned from an assessment of the lung apices. Findings of pulmonary edema include interlobular septal thickening and nodular or confluent ground-glass opacities, which are often accompanied by pleural effusions (Fig E12). This information can be helpful to the emergency and admitting physicians, particularly when the diagnosis was not made at chest radiography.

Superior Mediastinum

Typically, the area imaged at neck CT extends inferiorly as far as the aortic arch and therefore

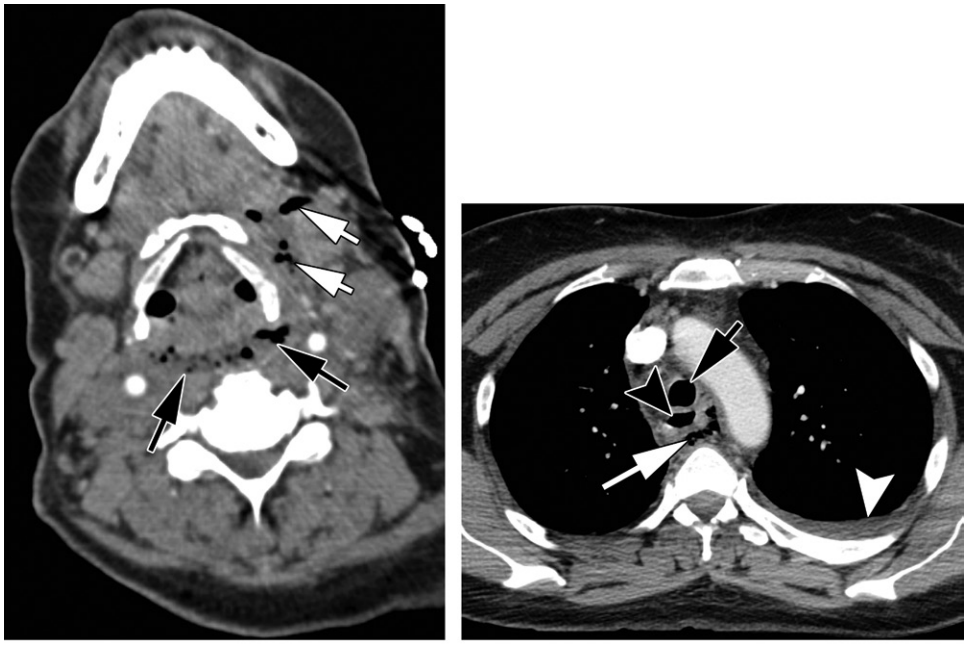

a. b.

Figure 25. Descending mediastinitis in a 50-year-old woman who recently underwent a dental procedure. **(a)** Axial contrast-enhanced CT image shows foci of gas and fluid (white arrows) in the left submandibular space, with extension to the danger space (black arrows). **(b)** Axial contrast-enhanced CT image obtained inferior to **a** shows continued extension into the mediastinum (white arrow) and a small left pleural effusion (white arrowhead). The trachea (black arrow) and esophagus (black arrowhead) also are seen.

includes the superior mediastinum. Visualized structures include the trachea, esophagus, aortic arch, and arch vessels, as well as the distal internal jugular veins, brachiocephalic veins, and superior vena cava. Under normal circumstances, the superior mediastinal fat should be homogeneous, without fat stranding or a pneumomediastinum. Residual thymic tissue should not be confused for disease, particularly in children and young adults (71). The vessels should exhibit normal opacification, without filling defects. The esophageal wall should not be thickened.

Suspected oropharyngeal or dental infection is a common indication for neck CT. Rarely, such infections extend into the mediastinum and result in a life-threatening complication known as descending necrotizing mediastinitis. The longitudinal orientation of the deep cervical fascia allows routes of infection spread from the head and neck into the mediastinum. The danger space is a well-described potential space between the alar fascia anteriorly and the prevertebral fascia posteriorly. It extends from the skull base to the diaphragm, through which head and neck infection can extend into the mediastinum (24). CT findings of descending necrotizing mediastinitis include fat stranding, myositis, mediastinal fluid collections, pleural and pericardial fluid collections, cervical adenopathy, and vascular thrombosis (Fig 25) (72,73).

Important aortic disease can be detected incidentally at neck CT performed in the emergency department. The incidental discovery and reporting of a thoracic aortic aneurysm seen on a neck CT image can affect the long-term survival of the patient (Fig E13) (74). Aortic dissections, penetrating ulcers, and large atheromas are other aortic pathologic conditions that can be seen at neck CT and are important to recognize. Mediastinal masses also may be detected on neck CT scans. Noting an anterior mediastinal mass in a patient with cervical adenopathy can help the clinician diagnose lymphoma. Goiters with mediastinal extension, thymomas, congenital cysts, esophageal masses, and neurogenic tumors are among the most common mediastinal masses that can be discovered incidentally at neck CT.

Synthesis of Findings

After specific findings are evaluated and reported in the proper sections of the report, the "Impression" section provides the opportunity to synthesize these findings into a unified diagnosis (Figure E14). The diagnosis of Lemierre syndrome (discussed earlier) is used to illustrate this synthesis process (Figure E15). Subcutaneous edema of the involved side should be included in the "Cutaneous and Subcutaneous Soft Tissues" section. The primary infection—for example, tonsillitis—is included in the "Aerodigestive Tract" section. Vascular clot or occlusion should be included in the "Vascular Structures" section.

Septic pulmonary emboli should be included in the "Lung Apices" section. These findings are merged in the "Impression" section, with the final diagnosis being Lemierre syndrome (Figure E15).

Conclusion

CT findings of the neck should be interpreted systematically, in a manner similar to that used to interpret other radiologic studies, such as abdominopelvic CT images and chest radiographs. The described approach involving evaluation of the 12 areas listed in Table 1 is recommended, particularly for the evaluation of acute infectious or inflammatory processes. Findings in these individual areas can then be synthesized into a coherent impression that describes the source and relationship of the disease in individual areas. Interpreting imaging findings in this fashion enables consistent identification of all findings and clear reporting of the disease process.

References

1. Giannitto C, Esposito AA, Casiraghi E, Biondetti PR. Epidemiological profile of non-traumatic emergencies of the neck in CT imaging: our experience. Radiol Med (Torino) 2014;119(10):784–789.
2. Maroldi R, Farina D, Ravanelli M, Lombardi D, Nicolai P. Emergency imaging assessment of deep neck space infections. Semin Ultrasound CT MR 2012;33(5):432–442.
3. Gamss C, Gupta A, Chazen JL, Phillips CD. Imaging evaluation of the suprahyoid neck. Radiol Clin North Am 2015;53(1):133–144.
4. Vieira F, Allen SM, Stocks RM, Thompson JW. Deep neck infection. Otolaryngol Clin North Am 2008;41(3):459–483, vii.
5. Marco De Lucas E, Sádaba P, Lastra García-Barón P, et al. Value of helical computed tomography in the management of upper esophageal foreign bodies. Acta Radiol 2004;45(4):369–374.
6. Ginat DT, Schatz CJ. Imaging features of midface injectable fillers and associated complications. AJNR Am J Neuroradiol 2013;34(8):1488–1495.
7. Sudhoff H, Rajagopal S, Mani N, Moumoulidis I, Axon PR, Moffat D. Usefulness of CT scans in malignant external otitis: effective tool for the diagnosis, but of limited value in predicting outcome. Eur Arch Otorhinolaryngol 2008;265(1):53–56.
8. Rosenfeld RM, Schwartz SR, Cannon CR, et al. Clinical practice guideline: acute otitis externa. Otolaryngol Head Neck Surg 2014;150(1 Suppl):S1–S24.
9. Michalowicz M, Ramanathan M Jr. Clival osteomyelitis presenting as a skull base mass. J Neurol Surg Rep 2017;78(2):e93–e95.
10. Rubin J, Curtin HD, Yu VL, Kamerer DB. Malignant external otitis: utility of CT in diagnosis and follow-up. Radiology 1990;174(2):391–394.
11. Koeller KK, Alamo L, Adair CF, Smirniotopoulos JG. Congenital cystic masses of the neck: radiologic-pathologic correlation. RadioGraphics 1999;19(1):121–146; quiz 152–153.
12. Adams A, Mankad K, Offiah C, Childs L. Branchial cleft anomalies: a pictorial review of embryological development and spectrum of imaging findings. Insights Imaging 2016;7(1):69–76.
13. Seeburg DP, Baer AH, Aygun N. Imaging of Patients with Head and Neck Cancer: From Staging to Surveillance. Oral Maxillofac Surg Clin North Am 2018;30(4):421–433.
14. Kelly HR, Curtin HD. Chapter 2 Squamous Cell Carcinoma of the Head and Neck: Imaging Evaluation of Regional Lymph Nodes and Implications for Management. Semin Ultrasound CT MR 2017;38(5):466–478.
15. Razek AA, Huang BY. Soft tissue tumors of the head and neck: imaging-based review of the WHO classification. RadioGraphics 2011;31(7):1923–1954.
16. Baxter FJ, Dunn GL. Acute epiglottitis in adults. Can J Anaesth 1988;35(4):428–435.
17. Charles R, Fadden M, Brook J. Acute epiglottitis. BMJ 2013;347:f5235.
18. Lee SH, Yun SJ, Kim DH, Jo HH, Ryu S. Do we need a change in ED diagnostic strategy for adult acute epiglottitis? Am J Emerg Med 2017;35(10):1519–1524.
19. Berger G, Landau T, Berger S, Finkelstein Y, Bernheim J, Ophir D. The rising incidence of adult acute epiglottitis and epiglottic abscess. Am J Otolaryngol 2003;24(6):374–383.
20. Smith MM, Heubi CH. Infections of the Neck and Pharynx in Children. Curr Treat Options Pediatr 2018;4(2):211–220.
21. Scott PM, Loftus WK, Kew J, Ahuja A, Yue V, van Hasselt CA. Diagnosis of peritonsillar infections: a prospective study of ultrasound, computerized tomography and clinical diagnosis. J Laryngol Otol 1999;113(3):229–232.
22. Ali SA, Kovatch KJ, Smith J, et al. Predictors of intratonsillar versus peritonsillar abscess: A case-control series. Laryngoscope 2019;129(6):1354–1359.
23. Lo CC, Luo CM, Fang TJ. Aberrant internal carotid artery in the mouth mimicking peritonsillar abscess. Am J Emerg Med 2010;28(2):259.e5–259.e6.
24. Hoang JK, Branstetter BF 4th, Eastwood JD, Glastonbury CM. Multiplanar CT and MRI of collections in the retropharyngeal space: is it an abscess? AJR Am J Roentgenol 2011;196(4):W426–W432.
25. Brucker JL, Gentry LR. Imaging of head and neck emergencies. Radiol Clin North Am 2015;53(1):215–252.
26. Chalifoux JR, Vachha B, Moonis G. Imaging of Head and Neck Infections: Diagnostic Considerations, Potential Mimics, and Clinical Management. Semin Roentgenol 2017;52(1):10–16.
27. Offiah CE, Hall E. Acute calcific tendinitis of the longus colli muscle: spectrum of CT appearances and anatomical correlation. Br J Radiol 2009;82(978):e117–e121.
28. Ishigami K, Averill SL, Pollard JH, McDonald JM, Sato Y. Radiologic manifestations of angioedema. Insights Imaging 2014;5(3):365–374.
29. Nandi P, Ong GB. Foreign body in the oesophagus: review of 2394 cases. Br J Surg 1978;65(1):5–9.
30. Prabhu SM, Irodi A, George PP, Sundaresan R, Anand V. Missed intranasal wooden foreign bodies on computed tomography. Indian J Radiol Imaging 2014;24(1):72–74.
31. Scheinfeld MH, Shifteh K, Avery LL, Dym H, Dym RJ. Teeth: what radiologists should know. RadioGraphics 2012;32(7):1927–1944.
32. Merchant AT, Virani SS. Evaluating periodontal treatment to prevent cardiovascular disease: challenges and possible solutions. Curr Atheroscler Rep 2017;19(1):4.
33. Sakamoto H, Aoki T, Kise Y, Watanabe D, Sasaki J. Descending necrotizing mediastinitis due to odontogenic infections. Oral Surg Oral Med Oral Pathol Oral Radiol Endod 2000;89(4):412–419.
34. Som PM, Curtin HD. Fascia and spaces of the neck. In: Som PM, Curtin HD, eds. Head and neck imaging. 5th ed. St Louis, Mo: Mosby, 2011; 2203–2234.
35. Yu CH, Minnema BJ, Gold WL. Bacterial infections complicating tongue piercing. Can J Infect Dis Med Microbiol 2010;21(1):e70–e74.
36. Kumbhar SS, O'Malley RB, Robinson TJ, et al. Why thyroid surgeons are frustrated with radiologists: lessons learned from pre- and postoperative US. RadioGraphics 2016;36(7):2141–2153.
37. Nachiappan AC, Metwalli ZA, Hailey BS, Patel RA, Ostrowski ML, Wynne DM. The thyroid: review of imaging features and biopsy techniques with radiologic-pathologic correlation. RadioGraphics 2014;34(2):276–293.
38. Tessler FN, Middleton WD, Grant EG. Thyroid Imaging Reporting and Data System (TI-RADS): A User's Guide. Radiology 2018;287(1):29–36.
39. Bin Saeedan M, Aljohani IM, Khushaim AO, Bukhari SQ, Elnaas ST. Thyroid computed tomography imaging:

pictorial review of variable pathologies. Insights Imaging 2016;7(4):601–617.
40. Paquette CM, Manos DC, Psooy BJ. Unilateral vocal cord paralysis: a review of CT findings, mediastinal causes, and the course of the recurrent laryngeal nerves. RadioGraphics 2012;32(3):721–740.
41. Yedla N, Pirela D, Manzano A, Tuda C, Lo Presti S. Thyroid abscess: challenges in diagnosis and management. J Investig Med High Impact Case Rep 2018;6:2324709618778709.
42. Johnson NA, Tublin ME, Ogilvie JB. Parathyroid imaging: technique and role in the preoperative evaluation of primary hyperparathyroidism. AJR Am J Roentgenol 2007;188(6):1706–1715.
43. Li RM, Kiemeney M. Infections of the Neck. Emerg Med Clin North Am 2019;37(1):95–107.
44. Abdel Razek AAK, Mukherji S. Imaging of sialadenitis. Neuroradiol J 2017;30(3):205–215.
45. Hoang JK, Vanka J, Ludwig BJ, Glastonbury CM. Evaluation of cervical lymph nodes in head and neck cancer with CT and MRI: tips, traps, and a systematic approach. AJR Am J Roentgenol 2013;200(1):W17–W25.
46. Ludwig BJ, Wang J, Nadgir RN, Saito N, Castro-Aragon I, Sakai O. Imaging of cervical lymphadenopathy in children and young adults. AJR Am J Roentgenol 2012;199(5):1105–1113.
47. Hanson RA, Thoongsuwan N. Scrofula. Curr Probl Diagn Radiol 2002;31(6):227–229.
48. Lee YY, Van Tassel P, Nauert C, North LB, Jing BS. Lymphomas of the head and neck: CT findings at initial presentation. AJR Am J Roentgenol 1987;149(3):575–581.
49. Saba L, Sanfilippo R, Montisci R, Suri JS, Mallarini G. Carotid artery wall thickness measured using CT: inter- and intraobserver agreement analysis. AJNR Am J Neuroradiol 2013;34(2):E13–E18.
50. Saba L, Anzidei M, Sanfilippo R, et al. Imaging of the carotid artery. Atherosclerosis 2012;220(2):294–309.
51. Rodallec MH, Marteau V, Gerber S, Desmottes L, Zins M. Craniocervical arterial dissection: spectrum of imaging findings and differential diagnosis. RadioGraphics 2008;28(6):1711–1728.
52. Lecler A, Obadia M, Savatovsky J, et al. TIPIC Syndrome: Beyond the Myth of Carotidynia, a New Distinct Unclassified Entity. AJNR Am J Neuroradiol 2017;38(7):1391–1398.
53. Vlak MH, Algra A, Brandenburg R, Rinkel GJ. Prevalence of unruptured intracranial aneurysms, with emphasis on sex, age, comorbidity, country, and time period: a systematic review and meta-analysis. Lancet Neurol 2011;10(7):626–636.
54. Eilbert W, Singla N. Lemierre's syndrome. Int J Emerg Med 2013;6(1):40.
55. Som PM, Brandwein MS, Wang BY. Inflammatory disease of the sinonasal cavities. In: Som PM, Curtin HD, eds. Head and neck imaging. 5th ed. St Louis, Mo: Mosby, 2011; 167–251.
56. Wyler B, Mallon WK. Sinusitis Update. Emerg Med Clin North Am 2019;37(1):41–54.
57. Aribandi M, McCoy VA, Bazan C 3rd. Imaging features of invasive and noninvasive fungal sinusitis: a review. RadioGraphics 2007;27(5):1283–1296.
58. Middlebrooks EH, Frost CJ, De Jesus RO, Massini TC, Schmalfuss IM, Mancuso AA. Acute Invasive Fungal Rhinosinusitis: A Comprehensive Update of CT Findings and Design of an Effective Diagnostic Imaging Model. AJNR Am J Neuroradiol 2015;36(8):1529–1535.
59. Montone KT. Pathology of fungal rhinosinusitis: a review. Head Neck Pathol 2016;10(1):40–46.
60. Vazquez E, Castellote A, Piqueras J, et al. Imaging of complications of acute mastoiditis in children. RadioGraphics 2003;23(2):359–372.
61. Ludwig BJ, Foster BR, Saito N, Nadgir RN, Castro-Aragon I, Sakai O. Diagnostic imaging in nontraumatic pediatric head and neck emergencies. RadioGraphics 2010;30(3):781–799.
62. Tali ET, Oner AY, Koc AM. Pyogenic spinal infections. Neuroimaging Clin N Am 2015;25(2):193–208.
63. Morales H. Infectious Spondylitis Mimics: Mechanisms of Disease and Imaging Findings. Semin Ultrasound CT MR 2018;39(6):587–604.
64. Egerter AC, Kim ES, Lee DJ, et al. Dysphagia Secondary to Anterior Osteophytes of the Cervical Spine. Global Spine J 2015;5(5):e78–e83.
65. Nguyen VD, Singh AK, Altmeyer WB, Tantiwongkosi B. Demystifying orbital emergencies: A pictorial review. RadioGraphics 2017;37(3):947–962.
66. Absoud M, Hikmet F, Dey P, Joffe M, Thambapillai E. Bilateral cavernous sinus thrombosis complicating sinusitis. J R Soc Med 2006;99(9):474–476.
67. Expert Panel on Neurologic Imaging:, Kennedy TA, Corey AS, et al. ACR Appropriateness Criteria: Orbits Vision and Visual Loss. J Am Coll Radiol 2018;15(5S):S116–S131.
68. Ziegler A, Patadia M, Stankiewicz J. Neurological Complications of Acute and Chronic Sinusitis. Curr Neurol Neurosci Rep 2018;18(2):5.
69. Self WH, Courtney DM, McNaughton CD, Wunderink RG, Kline JA. High discordance of chest x-ray and computed tomography for detection of pulmonary opacities in ED patients: implications for diagnosing pneumonia. Am J Emerg Med 2013;31(2):401–405.
70. Monnier-Cholley L, Arrivé L, Porcel A, et al. Characteristics of missed lung cancer on chest radiographs: a French experience. Eur Radiol 2001;11(4):597–605.
71. Drabkin MJ, Meyer JI, Kanth N, et al. Age-stratified patterns of thymic involution on multidetector CT. J Thorac Imaging 2018;33(6):409–416.
72. Scaglione M, Pinto A, Giovine S, Di Nuzzo L, Giuliano V, Romano L. CT features of descending necrotizing mediastinitis: a pictorial essay. Emerg Radiol 2007;14(2):77–81.
73. Capps EF, Kinsella JJ, Gupta M, Bhatki AM, Opatowsky MJ. Emergency imaging assessment of acute, nontraumatic conditions of the head and neck. RadioGraphics 2010;30(5):1335–1352.
74. Kuzmik GA, Sang AX, Elefteriades JA. Natural history of thoracic aortic aneurysms. J Vasc Surg 2012;56(2):565–571.